International Institute for
Applied Systems Analysis
IIASA www.iiasa.ac.at

Contaminant Plume Migration in an Aquifer: Finite Element Modeling for the Analysis of Remediation Strategies: A Case Study

Diersch, H.J. and Kaden, S.

IIASA Collaborative Paper
April 1984

CONTAMINANT PLUME MIGRATION IN AN AQUIFER: FINITE ELEMENT MODELING FOR THE ANALYSIS OF REMEDIATION STRATEGIES: A CASE STUDY

H.-J. Diersch
S. Kaden

April 1984
CP-84-11

INTERNATIONAL INSTITUTE FOR APPLIED SYSTEMS ANALYSIS
2361 Laxenburg, Austria

AUTHORS

Hans-Jörg Diersch is from the Institute for Mechanics of the Academy of Sciences of the German Democratic Republic, Berlin.

Stefan Kaden is with the Regional Water Policies project of the Institutions and Environmental Policies Program at the International Institute for Applied Systems Analysis, Laxenburg, Austria.

PREFACE

Intense regional development in many parts of the world creates an increasing pressure on the environment both by consuming natural resources and by discharging wastes that are hazardous to the population and to natural ecosystems. A substantial part of these interactions between regional socio-economic and environmental systems takes place through regional groundwater systems. Apart from being the resource that is highly vital for socio-economic development and for the evolution of ecosystems, the regional groundwater system is often a basic medium through which local human interventions penetrate to and are "felt" in other parts of the region, and also frequently beyond its boundaries.

To study the role of natural groundwater systems in regional development and also regional policies capable of preventing further degradation of groundwater are one of the goals of the "Regional Water Policies" project at IIASA. One of the challenges in this research is to cope with the inherent complexity of "hidden" groundwater processes. Depending on the goals of a particular stage of the analysis models of varying sophistication should be used. This paper exemplifies the use of a rather elaborated model for the analysis of a relatively "local" scale of the means to prevent the spreading of contaminants in a groundwater aquifer. After discussing the model and its verification using field data, the authors make a comparative long-term analysis of 3 types of remediation strategies for a case region in the GDR.

S. Orlovski
Project Leader
Regional Water Policies

ABSTRACT

Groundwater resources are becoming more and more endangered of being depleted by over-exploitation and of being polluted as a consequence of environmentally insensitive economic activities and population growth in many regions and countries of the world.

Causes and consequences of quantitative and qualitative changes in groundwater states can be separated by decades and centuries. Once contaminated or depleted, groundwater resources may be permanently impaired. This fact becomes especially obvious in the case of groundwater pollution by hazardous wastes. Necessary remediation strategies may be extremely time and money consuming. Therefore, the optimal design of such remediation strategies is of great importance.

The paper describes the results of a case study dealing with historical and predictive modeling of the migration of a real contaminant plume in an alluvial aquifer threatening the nearby operating extraction wells for municipal water supply. As a modeling case study it primarily aims at modeling and examining current and intended remediation strategies. The consequences and benefits of a hydraulic barrier in continuous or intermittent operation and their combination with pumpage from interception wells are investigated and discussed.

For these purposes a horizontal plane transport model based on a finite element approach has been developed and applied. The model has been tested and calibrated through a history matching procedure comparing model computations with observed field data, where hydrodynamic dispersivities are identified as principal parameters. The obtained prognostic results allow several practical conclusions on the design of remediation strategies.

The used finite element model simulator FEFLOW has proved to be a convenient and powerful tool in modeling the complex flow and transport processes of the contaminant plume. It demonstrates the abilities in prospective simulations for decision purposes.

CONTENTS

CONTAMINANT PLUME MIGRATION IN AN AQUIFER: FINITE ELEMENT MODELING FOR THE ANALYSIS OF REMEDIATION STRATEGIES: A CASE STUDY

H.-J. Diersch and S. Kaden

1. Introduction

Groundwater resources are an increasingly important component of the regional development in many regions. General awareness about the importance of the precious groundwater resources has greatly extended in recent times. In many countries of the world, groundwater is valued for its high quality, its avaibility close to the user and its reliability, satisfying an important part of the drinking water supply.

Nowadays groundwater resources are becoming more and more endangered of being depleted by over-exploitation and of being polluted as a consequence of environmentally insensitive economic activities and population growth in many regions and countries of the world. The most important impacts on groundwater are caused by agriculture (e.g. nitrate pollution), industry (hazardous and toxic waste disposal, landfills, etc.), mining operations (especially open-cast mines), and drinking and irrigation water withdrawals.

Causes and consequences of quantitative and qualitative changes in groundwater regimes can be separated by decades or centuries. Once contaminated or depleted, groundwater resources may be permanently impaired. This is one of the most characteristic "creeping" problems, which calls

foremost for preventive actions and appropriate policies to avoid situations which are extremely difficult to cure and rectify. Groundwater degradation is progressing at such a speed that *groundwater depletion and pollution* is considered in many countries to be the *most important water-related problem* of the 80s.

The present paper deals with one special problem of groundwater degradation — the contamination due to hazardous wastes. Groundwater contamination, particularly from hazardous wastes, has been recognized as a very serious national problem in many countries (Wood et al. 1984). Our advanced technological society implies the increasing danger of chemical contamination throughout the environment, especially the soil and the groundwater resources. The number of potential solid and liquid contaminants of commercial and industrial wastes is tremendous and the number of serious groundwater contaminations from hazardous wastes is manifold (for instance, see Jackson et al. 1980, Wood et al. 1984). Such contaminations necessitate remediation measures above all in cases of aquifers being used for water supply. Different techniques for subsurface improvement of groundwater quality are available as for instance the pumpage of contaminated water, the building up of hydraulic barriers by the help of artificial recharge or subsurface water treatment technologies. All these techniques may be extremely time and money consuming and they have to be investigated frequently within the framework of regional water or more general environmental policies.

All these problems mentioned above explain a continuing and growing need for the analysis and design of regional policies capable of providing the rational use and protection of groundwater and surface water resources as well as the remediation of degraded resources.

The IIASA project "Regional Water Policies" aims at the elaboration of a conceptual framework, methodology, and computer-based methods, which can assist the analysis of such policies. Thereby, the groundwater resources have to be considered a part of the complex socio-economic and environmental systems. Consequently, modeling principles for groundwater subsystems should be developed, which focus on their links with economic, social and other processes pertinent to regional human activity. Due to the complexity of these links and the varying scale in space and time as well as the different modeling goals, hierarchical systems of models are required.

The range of models includes highly sophisticated multidimensional models with distributed parameters but also simplified models with lumped parameters. For modeling *groundwater flow*, appropriate models for almost all purposes are available. Difficulties arise in the case of modeling *groundwater quality*. Generally, a sophisticated modeling framework is used to simulate those complicated processes. The paper describes the use of such a rather elaborated model. Generalized methods for the development of simplified models based on the sophisticated models are not yet available.

The design of remediation strategies for contaminated aquifers is a typical problem which necessitates the use of sophisticated numerical models. In the following, the results of a methodological case study dealing with modeling the migration of an actual contaminant plume in an alluvial aquifer are described. The study was mainly directed towards examining current and intended remediation strategies. For the numerical modeling the finite element method has been used. By way of introduction, some theoretical development for numerical simulation of local groundwater contamination is given.

The paper characterises possibilities and bounds of sophisticated modeling for policy design. In conclusion, research needs from the point of view of the analysis and design of regional water policies are outlined.

2. Numerical Simulation of Local Groundwater Contamination

2.1. Background

In the following we assume that a contaminant plume consisting of relevant chemical components (contaminants) enters an aquifer or is located within it. The causes of the formation of the plume may be neglected. Dependent on the physical-chemical properties of the contaminants two fundamental different approaches are common:

- the *single phase* flow, considering a binary chemical system consisting of two miscible species (with similar density and viscosity): the solution characterised by the contaminant and the solvent water, which is assumed to be an ideal (or colloid) solution;

- the *multifluid* or *multiphase* flow of nonsoluble fluids with different density and viscosity.

The first approach (mixing or dilution) is applicable to a great class of inorganic and organic compounds, dependent on the solubility and the concentration of the contaminants. In this range, for instance nitrate, pesticides and phenols (see Zilliox et al. 1974) can be incorporated. We will concentrate on this approach below. The second approach is typical for petroleum and organic solvant contamination.

The movement of contaminants within porous media is called *migration* or *mass transport* processes.

The displacements and changes of chemical species in groundwater are governed and influenced by the following physical and chemical processes:

(1) convection [chemicals are moving (translating) with the flowing groundwater]

(2) hydrodynamic dispersion [spreading by physicochemical effects (molecular diffusion) and mechanical effects in the macroscopic scale of aquifer (hydromechanical dispersion)]

(3) medium-surface interaction of species [reaction between the dissolved species and the solid aquifer material (sorption)]

(4) mass change processes [chemical and/or biological processes within the mixture].

The description of these processes in a complex hydrogeological system with its geoscale spatial and temporal dimension is usually based on *deterministic models* describing the mass (including species concentration)and momentum conservation. (See, for instance, Bear 1972). Recently, stochastic modeling approaches are getting more consideration (Dagan 1983), forced by difficulties describing the scale dependent dispersion (see below). In developing the deterministic models, statistical averaging procedures are used to transform the pore-scale microscopic processes to the large scale (see, Hassanizadeh and Gray 1979). This leads to a system of macroscopic conservation equations valid for a given volume the so-called REV (representative elementary volume). Statistical influences are involved in parameter relations, primarily for the mechanical dispersion, incorporating the measure of heterogeneity (microscopic, macroscopic) of the medium or area (column, field or regional scale), as described below. As an essential consequence the transport

processes have to be treated in their real scales. For regional-scale transport, these processes are long-term, measured in the order of months or years. This emphasizes both, the restricted applicability of experiments and observations, and the necessary application of mathematical modeling.

The mathematical solution of the deterministic conservation equations for complicated problems can only be done numerically. Analytical solutions are known only for some special cases, often for one-dimensional transport (v. Genuchten et al. 1982, Voigt and Häfner 1983). Also, for numerical solutions the general three-dimensional migration processes are simplified to two-dimensional processes, due to the lack of data, the required accuracy and the computing effort. The movement of local groundwater contaminations (contaminant plumes) within aquifers usually is supposed to be a horizontal plane movement. The three-dimensional, sometimes nonlinear partial differential equations of the migration process can be transformed into two-dimensional vertically averaged equations (see, Gray 1982) based on the Dupuit assumptions.

Bredehoeft and Pinder (1973) developed horizontal aquifer transport equations which were utilized in modelling the groundwater contamination at Brunswick, Georgia, USA. To solve numerically the horizontal aquifer model *finite difference methods* and the *method of characteristics* were used. The same concept was applied by Konikow (1977) for an extensive contamination study of the Rocky Mountain Arsenal, near Denver, Colorado, USA. However, these numerical methods has been found to be unsuitable for some hydrodynamic situations commonly encountered in the field. The *finite element method* (e.g., Pinder and Gray 1977) has proved to be a more general (vis-a-vis ad hoc) simulation technique well suited to hydrogeological field problems in modeling realistic groundwater contamination, because of its flexibility and such inherent numerical properties as

(1) accurate approximation of velocity field (conservativity)

(2) accurate approximation regarding the species concentration to avoid relevant influences by numerical dispersion (unrealistic sloping and spreading of concentration waves or fronts)

(3) stable solution especially for significant convection.

The finite element method was used by Pinder (1973) to model practically the movement of a plume of contaminated groundwater on Long Island, New York. Further works concerning the modeling of contamination problems in groundwater can be found (e.g., Segol and Pinder 1976, Pickens and Grisak 1981b, Pinder and Gray 1977, Pickens and Lennox 1976, Mohsen et al. 1978, Diersch 1979, 1981a, Diersch and Nillert 1984a, Gray and Hoffman 1981, see also their references) demonstrating the advantageous performance. Galerkin-finite element formulations using time-weighted approximations (Crank-Nicolson and implicit schemes) have become prominent in the field. Upwind schemes for numerical stability have been used only in special cases because they can induce a great measure of false numerical dispersion. Locally exact upwind schemes developed for one-dimensional transport equations using finite differences and finite elements (Enquist and Kreiss 1979, Stoyan 1979) can also cause problems if extended to higher dimensional processes. Moreover, an investigation and discussion can be found e.g., in Diersch (1983b).

In mathematical simulation of species transport in groundwater an important problem is the approach and validation of representative parameters of aquifer dispersion in terms of dispersivities (Bertsch 1978, Fried 1975) that are macro-dispersivities. In general, field measurements are necessary due to the inability to describe the real groundwater system using the coefficients derived from laboratory experiments. Frequently well tracer experiments (e.g., Beims 1983, Hibsch and Kreft 1979) in the aquifer investigated are carried on. However, the application to large-scale contamination processes is not generally or only conditionally possible (see also Section 2.2). To overcome these difficulties it is usual in modeling practice to fit the numerical model to observed space-time concentration field distributions via historical epignosis (history match) simulations, e.g., Konikow (1977), Pinder (1973), Gray and Hoffman (1981), Das Gupta and Yapa (1982). This strategy is also used in the present study. Difficulties regarding this procedure can result from the multiparameter influence including the numerical accuracy of models and the time consumption of model fitting. Beims (1983) has attempted to empirically relate dispersivities to corresponding area scales, ranging from laboratory experiments to regional results as shown in Figure 1. However, it should be clear that even more so for regional contamination problems, these values can only be rough values due to field and model influences on macro-dispersivities.

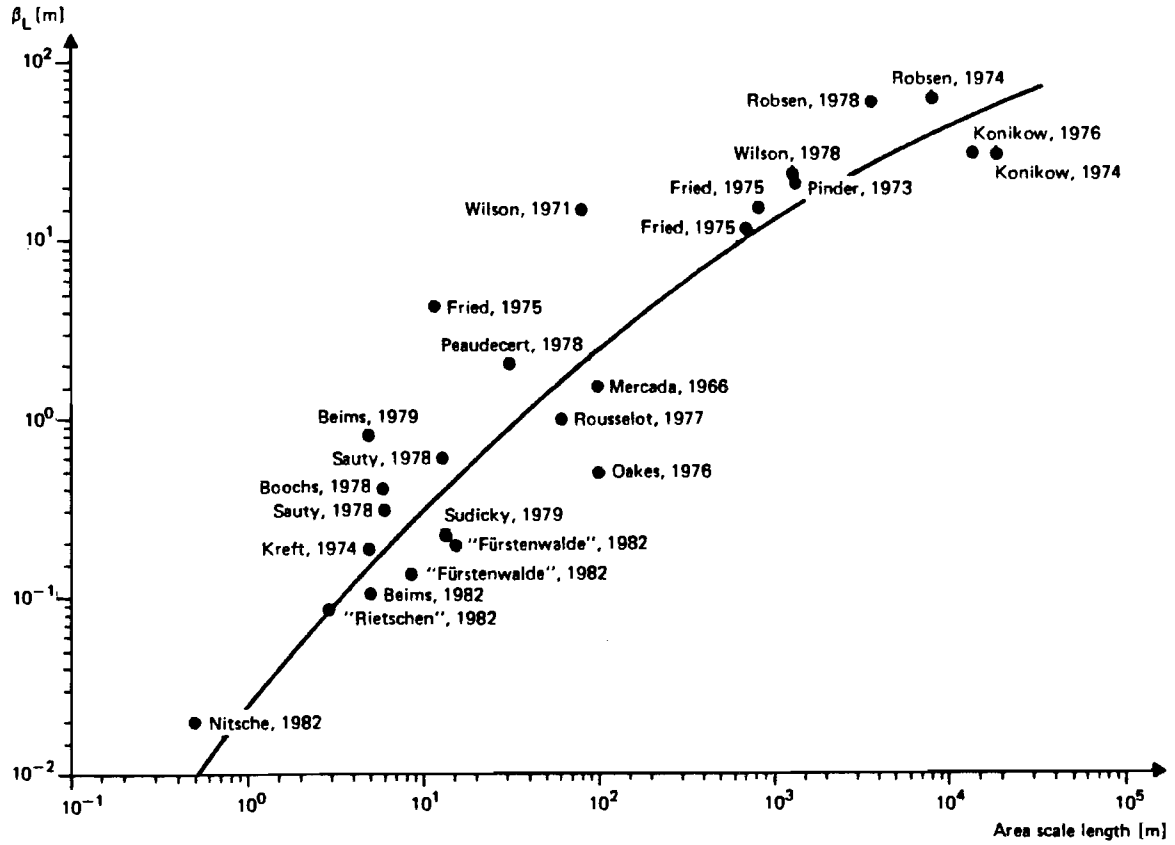

Figure 1. Dependence of longitudinal dispersivity on the area scale length, from Beims (1983)

To improve the representativeness and to generalize the dispersivity dependence within aquifers it has recently been attempted to describe the heterogeneity of aquifers by large-scale spatial distribution in hydraulic conductivity with geostatistical methods (Smith and Schwartz 1980). Here, the dispersivity becomes dependent on migration path (travel distance from the contaminant source) and the mean and variance of velocities (Tang et al. 1982). Pickens and Grisak (1981b) have shown that the distance-dependent dispersivities, however, are not important for long-term predictions.

Summarizing the discussion above, for the modeling of regional transport of a local contaminant plume, the following premises should be taken into account:

(1) Flow and transport processes are (at least) two-dimensional (horizontal).

(2) There is a large-scale spatial and temporal movement of the contaminant plume.

(3) The parameter estimation (dispersivities) has to be done via history match simulations.

(4) The finite element method should be used as the most general and accurate technique.

2.2. Basic Equations and Parameters

The flow and species transport processes in three-dimensional aquifer systems are described by the balance equations (summation convention is for $i,j = 1,2,3$), (Bear 1979, Diersch et al. 1983c) as follows:

$$S_s \frac{\partial h}{\partial t} + \frac{\partial}{\partial_i}(n v_i) = 0 \tag{1a}$$

with

$$S_s = \rho_o g (\alpha + n\beta) \tag{1b}$$

for conservation of groundwater mass,

$$v_i + \frac{K_{ij}}{n}\left(\frac{\partial h}{\partial x_j} + \frac{\rho-\rho_o}{\rho_o} e_j\right) = 0 \tag{2}$$

for momentum conservation of groundwater (generalized Dacy's law), and

$$\frac{\partial(nC)}{\partial t} + \frac{\partial(1-n)\cdot s}{\partial t} + \frac{\partial}{\partial x_i}(n v_i C) - \frac{\partial}{\partial x_i}\left(n D_{ij} \frac{\partial C}{\partial x_j}\right)$$

$$- n\lambda_o + \lambda_1[nC + (1-n)s] = 0 \tag{3a}$$

for conservation of species mass (transport equation) with

$$s = f(C) \tag{3b}$$

and

$$D_{ij} = (D_d + \beta_T V)\delta_{ij} + (\beta_L - \beta_T)\frac{v_i v_j}{V} \quad , \tag{3c}$$

where (see also Appendix C):

S_s = specific storage coefficient (L^{-1});

h = hydraulic head (L);

n = kinematic porosity (L^0);

v_i = components of average pore velocity (LT^{-1});

ρ = groundwater density (ML^{-3});

ρ_o = reference groundwater density (ML^{-3});

g = gravitational acceleration (LT^{-2});

α = skeleton compressibility (1);

β = compressibility of groundwater (1);

K_{ij} = tensor of hydraulic conductivity (LT^{-1});

e_j = components of gravitational unit vector in the direction x_j(1);

C = solute concentration of chemical component (ML^{-3});

s = solute concentration sorbed (ML^{-3});

D_{ij} = tensor of hydrodynamic dispersion (L^2T^{-1});

D_d = medium diffusion coefficient (L^2T^{-1});

β_l , β_T = coefficients of longitudinal and transverse dispersivity, respectively (L);

V = $(v_i v_i)^{1/2}$, absolute pore velocity (LT^{-1});

δ_{ij} = $\begin{cases} 1 & \text{for } i = j \\ 0 & \text{for } i \neq j \end{cases}$ Kronecker tensor

λ_0 = reaction term ($ML^{-3}T^{-1}$);

λ_1 = concentration decay rate (T^{-1}).

Considering regional flow fields where their horizontal extent dominates over the aquifer thickness the three-dimensional equations can be reduced to horizontal two-dimensional ones because vertical variations are generally not important compared with their horizontal dynamics, and can therefore be neglected. For deriving the representative horizontal flow and transport model the three-dimensional equations (1) to (3) are integrated in the vertical x_3-direction associated with an averaging process of the dependent variables C, h, and v_i as well as the remaining parameters in the form of

$$C \rightarrow \hat{C}(x_1,x_2,t) = \frac{1}{M}\int_M C(x_1,x_2,x_3,t)dx_3 \tag{4}$$

with M = aquifer thickness (L),

and analogous for $\hat{h},\hat{v}_i$ etc. using the Dupuit approximation. Accordingly, this leads for i,j = 1,2 to (see Bredehoeft and Pinder 1973, Scholz 1982, Diersch et al. 1983c)

$$S\frac{\partial \hat{h}}{\partial t} + \frac{\partial}{\partial x_i}(\bar{q}_i) = -Q + W \tag{5}$$

$$\bar{q}_i + T_{ij}\frac{\partial \hat{h}}{\partial x_j} = 0 \tag{6}$$

$$MR\frac{\partial \hat{C}}{\partial t} + S^*\hat{C}\frac{\partial \hat{h}}{\partial t} + \frac{\partial}{\partial x_i}(\hat{C}\bar{q}_i - n\bar{D}_{ij}\frac{\partial \hat{C}}{\partial x_j}) =$$

$$= -C'Q + C''W + M[n\lambda_0 - R\lambda_1\hat{C}] \tag{7}$$

with the aquifer storage coefficients

$$S = n_0 + S_s M$$

(8)

$$S^* = n_0 + (1 - n_0)\kappa + S_s M \quad ;$$

and

$$R = n + (1 - n)\kappa \tag{9}$$

as the retardation factor assuming a linear isotherm equilibrium absorption; further the specific Darcy flux

$$\bar{q}_i = M\, n\, \hat{v}_i \quad (L^2T^{-1}) \quad ; \tag{10}$$

and the well function

$$Q = \sum_{l=1}^{b} Q_B(x_l)\delta(x_1 - x_{1l}, x_2 - x_{2l}) \quad . \tag{11}$$

with

Q_B = discharge of single wells at $(x_{1l}, x_{2l})(L^3T^{-1})$
(withdrawal (sink) = positive sign)

b = number of wells

$\delta(\,)$ = Dirac delta function;

with the transmissivity

$$T_{ij} = K_{ij} M \quad (L^2T^{-1}) \tag{12}$$

and the tensor of aquifer macrodispersion

$$\bar{D}_{ij} = (D_d M + \beta_T \bar{V})\delta_{ij} + (\beta_L - \beta_T)\frac{\bar{q}_i \bar{q}_j}{\bar{V}} \tag{13}$$

where further

n_0 = drainable or fillable porosity (L^0);

W = groundwater accretion (LT^{-1});

κ = sorption coefficient (1);

C' = well-sink/source concentration (ML^{-3});

C'' = accretion-related input concentration (ML^{-3});

$\bar{V} =$ $(\bar{q}_i \bar{q}_i)^{1/2}$, absolute specific flux $(L^2 T^{-1})$.

The formulation is applied to an unconfined aquifer with assumption that the phreatic (free) surface is equal to the hydraulic head. Considering unconfined aquifer for all practical purposes one holds $n_0 \gg S_s M$. The equations for confined aquifer can be derived from above when using $S = S^* = S_s M$.

The practical modelling of contaminant migration in an aquifer is therefore attributed to the preliminary computation of hydraulic head $\hat{h}$ and the resulting Darcy fluxes $\bar{q}_i$ by solving the flow equations (5) and (6) incorporating the parameters

coefficient of storativity	S
sink-source relations	Q, W
transmissivity	T_{ij} ,

and the subsequent prediction of the contaminant concentration $\hat{C}$ in aquifer by solving the transport equation (7) associated with the parameters

aquifer thickness	M
porosity	n
sorption coefficient	κ
sink-source relations	$\lambda_1, \lambda_0, C', C''$
longitudinal and transverse dispersivity	β_L, β_T.

Extended beyond the usual hydraulic parameter data necessity, for migration studies parameters describing sorption and possible chemical/biological reactions as well as parameters of dispersivity quantifying the hydrodynamic dispersion (spreading, dilution) become of importance. These parameters depend on the chemical components considered and the material through which flow takes place as well as possibly on the chemical/biological environment in the aquifer. For conservative mobile components (e.g., salts, hydrocarbons and similar products) these actions do not play a role or are negligibly small. The dispersivity parameters give the quantitative measure of longitudinal and transverse spreading of species in groundwater caused by hydrodynamic actions resulting from, on the one hand, the microscopic heterogeneity of pore space and, on the other hand, the macroscopic heterogeneity (conductivity distribution) of aquifer. Normally, their effects exceed significantly the isotropic mixing intensities produced by molecular diffusion.

Therefore, under practical conditions it can be assumed $D_d = 0$.

The heterogeneity influence on dispersion is expressed by the scale of study area occurring (Pickens and Grisak 1981a, Klotz 1982a). So β_L is in the range of

0.01–3 cm	for laboratory scale (column experiments)
0.1 –2 m	for field scale (well injection tests)
2 –150 m	for regional scale (model history match)

(maximum values known 900 m!, Das Gupta and Yapa 1982).

2.3. Finite Element Simulator FEFLOW

For modeling of two-dimensional processes in porous media, the Academy of Sciences of the German Democratic Republic developed a finite element program system FEFLOW (Diersch 1980a). It has already been successfully applied to contaminant transport resulting from hazardous intrusion due to bankfiltration from a stream (Diersch and Nillert 1983a), to saltwater intrusion (upconing) below pumping wells (Diersch et al. 1984a, Diersch and Nillert 1984b), and to density-coupled intrusion processes (Diersch 1981b, 1981c). In the following this program and its mathematical foundation is outlined.

In context of the finite element method the entire flow domain Ω with its boundary Γ is subdivided into a finite number of subdomains Ω^e, called finite elements, each bounded by Γ^e. The unknown dependent variables are $\hat{h}, \bar{q}_i (i = 1,2)$ and $\hat{C}$. In the interest of simplicity their averaging symbols, introduced by equations (4) and (10), will be subsequently omitted and are approximated by the trial functions

$$h(x_i,t) \sim \tilde{h}(x_i,t) = N_l(x_i) H_l(t)$$

$$q_i(x_i,t) \sim \tilde{q}_i(x_i,t) = N_l(x_i) V_{il}(t) \qquad (14)$$

$$C(x_i,t) \sim \tilde{C}(x_i,t) = N_l(x_i) C_l(t)$$

with $i = 1,2$; $l = 1,2,\cdots,m$,

where N_l are basis functions and m corresponds to the number of discrete mesh-nodal points. For the present study biquadratic interpolation

expressions modelled by isoparametric curved eight-noded quadrilateral elements are used advocating a higher accuracy and flexibility.

The solution of the two-dimensional differential equations (5), (6) and (7) is based on a substitution model accomplished when the Darcy equation (6) is introduced into the continuity equation (5). Reducing to the solution of the primary unknowns h and C the computations are significantly simplified, as often practised, e.g., by Konikow (1977) and Pinder and Gray (1977). The necessary determination of velocities q_i (secondary unknowns) is here based on a derivative evaluation of the discrete h-fields applying the equations (6) and (14). Consequently, however, the conformity regarding q_i is no longer guaranteed which can lead to numerical errors under certain circumstances in zones with high velocity gradients. Accordingly, for some applications (Diersch 1981b,c) formulations in all primitive variables were preferred involving, however, a corresponding higher computational effort. Both ways can be applied via the user-oriented FEFLOW code developed (Diersch 1980a). The element type as used here with higher interpolation order seems to be an appropriate compromise between effort and velocity accuracy necessary for two-dimensional transport processes. In this case the velocities vary bilinearly over the element. As further outlined in Appendix A it follows superconvergent velocity dependences when using a suitable derivative concept.

The finite element model equations resulting from a Galerkin-version of method of weighted residuals (e.g., Pinder and Gray 1977) applied to equations (5), (6) and (7) and after using Green's theorem are given by

$$\int\int_{\Omega}(N\,S\,\frac{\partial h}{\partial t}+T_{ij}\,\frac{\partial N}{\partial x_i}\,\frac{\partial h}{\partial x_j})d\Omega = \tag{15}$$

$$= -\int\int_{\Omega}N(Q-W)\,d\Omega-\oint_{\Gamma}N\,q_h\,d\Gamma$$

and

$$\int\int_{\Omega}[N(M\,R\,\frac{\partial C}{\partial t}+\frac{\partial}{\partial x_i}(C\,q_i))+n\,D_{ij}\,\frac{\partial N}{\partial x_i}\,\frac{\partial C}{\partial x_j}+$$

$$+ N(R\ M\ \lambda_1 + S^* \frac{\partial h}{\partial t})C]d\Omega = \tag{16}$$

$$= -\int\int_{\Omega} N(C'Q - C''W - n\ M\ \lambda_0)d\Omega - \oint_{\Gamma} N\ q_c\ d\Gamma$$

where N represents the basic function $N_i(x_i)$ and

$$q_h = -T_{ij} \frac{\partial h}{\partial x_j} n_i$$

as well as

$$q_c = -n\ D_{ij} \frac{\partial C}{\partial x_j} n_i \tag{17}$$

correspond to the Darcy volumetric flux component and the concentration flux in normal direction positive outward to boundary Γ to be assigned, respectively; n_i are the directional cosines.

The following initial (I.C.) and boundary (B.C.) conditions hold:

Hydraulic head h

I.C. $h(x_i,0) = h_0(x_i,0)$

B.C. $h(x_i,t) = h_1^R$ on $\Gamma_1 \times t[0,\infty)$

(first kind or Dirichlet boundary condition)

$q_h = q_h^R$ on $\Gamma_2 \times t[0,\infty)$

(second kind or Neumann boundary condition)

$q_h = \Lambda_1(h_2^R - h)$ on $\Gamma_3 \times t[0,\infty)$

(third kind or Cauchy boundary condition)

Concentration C

I.C. $C(x_i,0) = C_0(x_i,0)$

B.C. $C(x_i,t) = C_1^R$ on $\Gamma_4 \times t[0,\infty)$

(first kind or Dirichlet boundary condition)

$q_c = q_c^R$ on $\Gamma_5 \times t[0,\infty)$

(second kind or Neumann boundary condition)

$q_c = \Lambda_2(C_2^R - C)$ on $\Gamma_6 \times t[0,\infty)$

(third kind or Cauchy boundary condition).

where $\Gamma_1 \cup \Gamma_2 \cup \Gamma_3 = \Gamma_4 \cup \Gamma_5 \cup \Gamma_6 = \Gamma$, the values identified by $\dot{R}$ designate prescribed boundary ones for the hydraulic head and concentration, Λ_1 and Λ_2 indicate aquifer-surface water interactions and concentration transfer coefficients, respectively.

After introducing equations (14) into (15) and (16) one finally obtains systems of algebraic equations, as described in Appendix A (equations (A11) and (A12)). These equations can be written symbolically in matrix form as follows:

$$\mathbf{A} \cdot \mathbf{H}_{t+\Delta t} = \mathbf{B} \cdot \mathbf{H}_t + \mathbf{G}_{t+\Delta t} \tag{18}$$

$$\mathbf{W} \cdot \mathbf{C}_{t+\Delta t} = \mathbf{E} \cdot \mathbf{C}_t + \mathbf{F}_{t+\Delta t} \tag{19}$$

when using a time-weighted difference scheme, where **H** and **C** are vectors containing the nodal unknowns for hydraulic head and concentration, and Δt represents the time step. The necessary "velocity"-field **V** is computed via a numerical derivation of the H-solution according to equation (6) and (A7), respectively. The structure of these matrices and vectors as well as the properties of schemes are further described in Appendix A.

Because chemical transport is much slower than momentum transport, for long-term quality simulations short-term perturbations in groundwater flow may be neglected and the groundwater flow be considered steady state as indicated below. In such cases, equation (18) reduces to (Appendix A)

$$\mathbf{T} \cdot \mathbf{H} = \mathbf{Y} \quad . \tag{20}$$

In Appendix A, appropriate singular well elements proposed by Charbeneau and Street (1979a,b) are introduced, being a combination of the local analytical well equation with numerical field solution allowing groundwater-flow fields near well-(point) singularities to model advantageously. They will be used especially in subsequent simulating the interception pumping of the contaminant plume (see Section 3.3.2.3).

To solve the symmetric and unsymmetric equation systems the FORTRAN-coded finite element program FEFLOW (Diersch 1980a) utilizes effective profile (envelope) and front elimination techniques. The present simulations were run on a BESM-6 computer.

3. The Case Study

3.1. Description of the Contamination Problem

In the vicinity of a drinking water supply station in the GDR, a groundwater contamination problem exists. Due to the destruction of an industrial plant in World War II a great quantity of organic contaminants were released and migrated to the underlying alluvial aquifer leading to a significant contamination of the groundwater resource in this area. As illustrated in Figure 2a, a contaminant plume has been observed within the groundwater basin of the drinking water supply station.

The pumping wells of the drinking water supply station obtain fresh groundwater from the northern tableland and infiltrated water from adjacent lakes in the east and the south. The study area is bounded to the west by a subsurface watershed. Due to this hydrogeologic setting and the increasing of pumping contaminated groundwater moved on an ever increasing scale toward the pumping well gallery *A*, posing a severe threat to water supply. The qualitative development of the pumping capacity is shown in Figure 3.

Recognizing the potential danger to public water supply, several field investigations and sampling of the contaminated area were carried out. In order to meet the demand, new pumping wells of the gallery *A* had to be constructed in the western part while the eastern wells exposed to the contaminant plume were becoming increasingly affected by the contamination and had to be partially taken out of action. In this period, at the beginning of the seventies, an extensive increase of contaminant concentration in the exposed wells (the well section (SWS) as indicated in Figures 2a and 4) was observed.

By this time the contaminant plume had expanded to about 1000 m in length and a width of between 130 m and 300 m as shown in Figures 2a and 5. There was only a relatively short distance of the plume from the SWS (see Figure 5). First assessments concerning a protection of the water supply wells

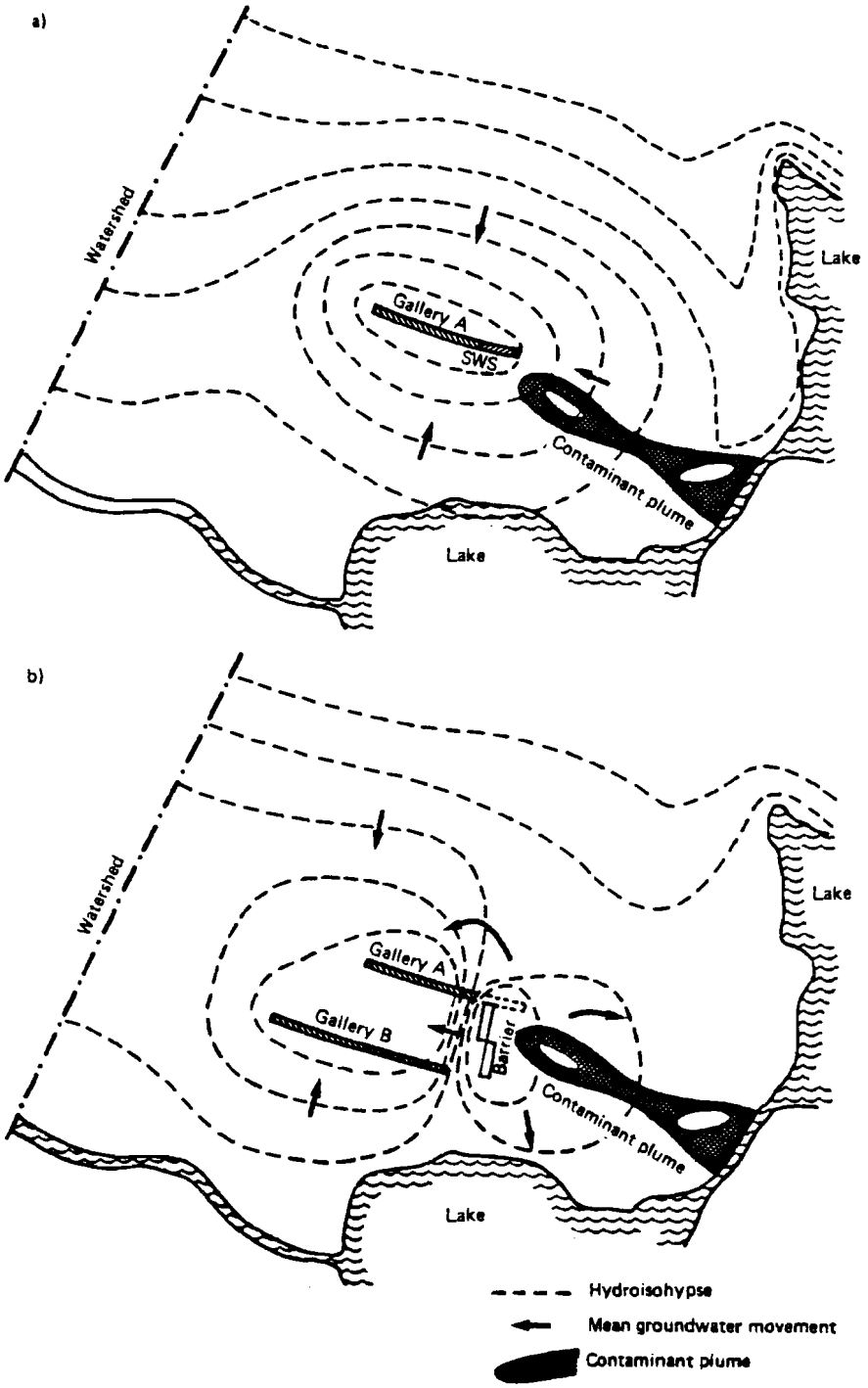

Figure 2. Location of the contaminant plume

a) Migration of the plume toward the supply wells (period from 1945 to 1977)

b) Intercepting the supply wells by an infiltration basin (period from 1977)

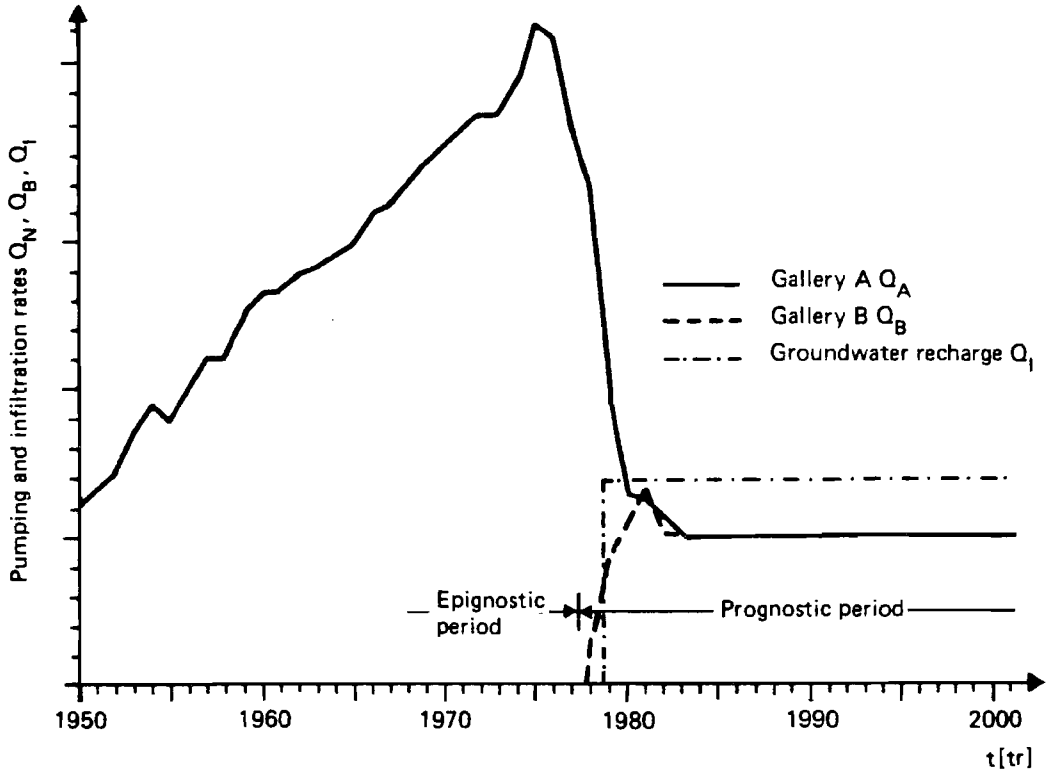

Figure 3. Development of day-averaged pumping rate (including basin infiltration) for the galleries of the drinking water supply station.

were devised. These assessments were connected with planning a second pumping well gallery B (see Figure 2b), required by an augmented water supply. To control the contamination, an infiltration basin has been proposed which should be capable of both intercepting the flow of contaminated groundwater towards the extraction wells and compensating the fresh groundwater losses due to the reduced groundwater resources. Its dual functions regarding a hydraulic barrier and an artificial groundwater recharge are shown in Figure 2b. The groundwater flow field is relatively complicated, having regions with different flow travelling both toward and away from the adjacent lakes, and areas with virtually no groundwater movement (in the eastern part of study area). Previously, the investigations concerning the location and design of the infiltration basin only resorted to mathematical modeling of the regional flows.

In 1978 the hydraulic barrier was installed. At the same time gallery B was put into operation. Since 1975 the pumping rate of the gallery A has decreased successively as indicated in Figure 3. At present its level equals gallery B's capacity. In the future we expect that this level for pumping (Figure 3) will be maintained.

Hydraulic modeling studies concerning the movement of the contaminant plume alone are adequate for making administrative, judicial, and public decisions on the control and assurance of groundwater quality and management of the supply station. Although the performance of the hydraulic barrier can be evaluated using hydraulic models, for a detailed prediction of the contaminant plume both, the advective and hydrodynamic dispersive behaviour of the contaminant plume have to be considered.

In determining the performance and benefits of the hydraulic barrier, the following aspects are of special interest

(i) the spatial and temporal distribution of the contaminant plume,

(ii) the duration of contaminant removal,

(iii) the rate that the contaminant (effluent) is entering the adjacent surface waters,

(iv) the endangering of uncontrolled flow of contaminated groundwater removing to the gallery or short-circuit travelling around the hydraulic barrier.

The present paper as a modeling case study deals with these problems on how the system operates. A further objective of this study is to investigate other remedial schemes and strategies of intercepting the contaminant plume. Potential strategies include:

(v) the intermittent operation of the hydraulic barrier, and

(vi) the pumping of the contaminated groundwater.

The model studies can be subdivided into phases:

(1) fitting the observed contamination (history matching)

(2) the prediction for contaminant interception and aquifer remediation.

The first phase serves as a calibration of the transport model developed in Section 3.2. For this use, historical data in the study area are available. The model is tested and calibrated through a history matching procedure comparing model computations with the observed contaminant breakthrough in the SWS up to its abandonment (see Figure 10). This period covers the years from 1968 through 1977. The principal parameter which had to be identified in the calibration process is the hydrodynamic dispersion.

The prediction phase begins in 1978, the date of starting the hydraulic barrier, and aims at the simulation and evaluation of interception and remediation activities. The simulation results are presented and discussed in Section 3.3. In Section 3.4 some conclusions are given.

3.2. The Transport Model

3.2.1. Hydrogeologic And Hydrochemical Description

3.2.1.1. Groundwater Flow

The study area is located in the sand formation of a primeval stream valley. Sand sequences attain relatively large thicknesses ranging between 30 and 60 m. The sand beds are underlain by silt, silty sand and clay. In the western part lenses of boulder marl and silt are interbedded locally. The hydrogeologic exploration leads to primary data regarding the aquifer properties and the hydraulic regime. Concerning a model-adequate assortment of data bases the present study relies on the hydrogeologic parameters estimated in previous research of the Institute for Water Management. According to a hydrogeological schematization regarding the aquifer thickness M and the isotropic transmissivity T the study area can be primarily subdivided into four subregions exhibited in Figure 4. The aquifer thicknesses and transmissivities specified subregionally are summarized in Appendix B.

For the porosity n a uniform value of 30% is assumed because no direct measurements were available. Assumptions regarding the storativity $S(=S^*)$ of about 0.20 and the groundwater recharge W of about 10.5 mm/month are based on previous research. In the case of interception pumping of the contaminant plume, it is intended to use single wells each with capacity 1000 m^3/day.

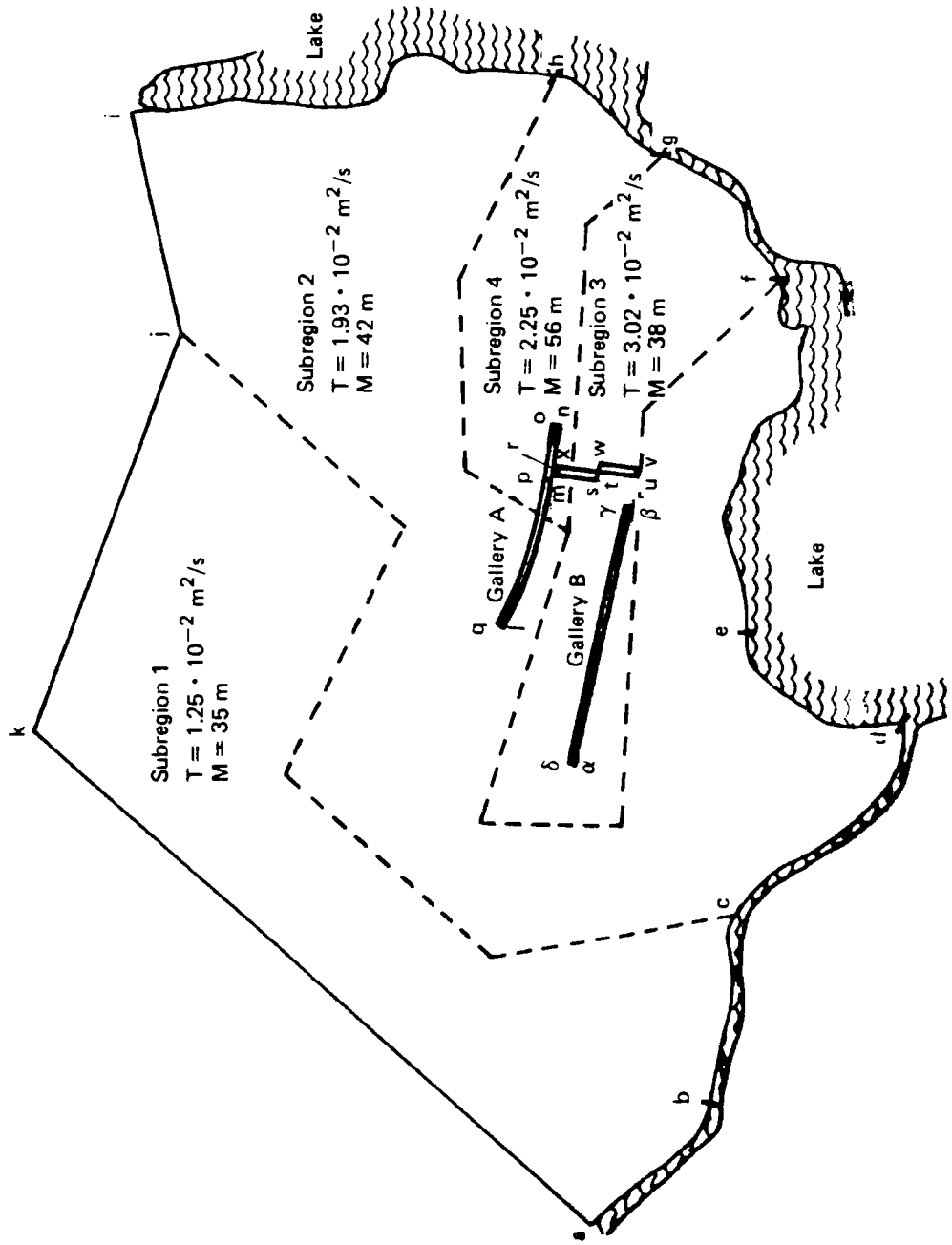

Figure 4. Hydrogeological schematization of study area.

3.2.1.2. Contaminant Migration

At the end of the 1960's observation wells were drilled to quantify the subsurface contamination in the area. The test wells characterizing the contaminant plume are indicated in Figure 5, only 12 test wells are available. To quantify the effective contaminant concentration within the plume five well samples are available as shown in Figure 5.

The contaminant measurements designate over the depth of the aquifer a concentration distribution varying in some cases quite drastically. The reasons for this are essentially unclear. According to horizontal modeling of the groundwater contamination problem, a depth-weighted vertical averaging of contaminant concentration is performed. The resulting concentration means for the wells are given in Figure 5. From the available measurements there is an areal extent of the contaminant plume at 1968 as displayed in Figure 5.

The measurements carried out in the subsequent years have referred to both selected test wells and producing wells. However, the observations are not systematic and the results have proved essentially to be unsuitable for characterization of the plume velocity. On the other hand, certain continuous field data have been available directly for the supply station wells. Here, the measured contaminant concentrations in the SWS of the gallery *A* exposed to the contaminant plume are of particular interest.

The measured contaminant breakthroughs into the wells of SWS in the 1970's up to their abandonments are shown later in Figure 10 (p. 36) concerning maximum and year-averaged mean concentrations normalized. Obviously, to calibrate the mathematical model the breakthrough characteristic of SWS appears to be best suitable due to its complete and unambiguous description and to be essentially the only possibility compared with the remaining contaminant data available. In the sense of a conservative fitting, the model fitting should be based on measured maximum contaminant values.

To model the contaminant migration the dispersivities β_L and β_T have to be estimated. According to the regional extent of the contaminant plume, for the present investigations ranging from several hundred meters up to one thousand meters, the longitudinal dispersivity β_L is expected to be in the range between 3 and 12 m (see Figure 1). However finally, the representative value can be primarily obtained by an appropriate historical model adaption

ϕ = Depth-weighted mean contaminant concentration normalized by C_{ref}

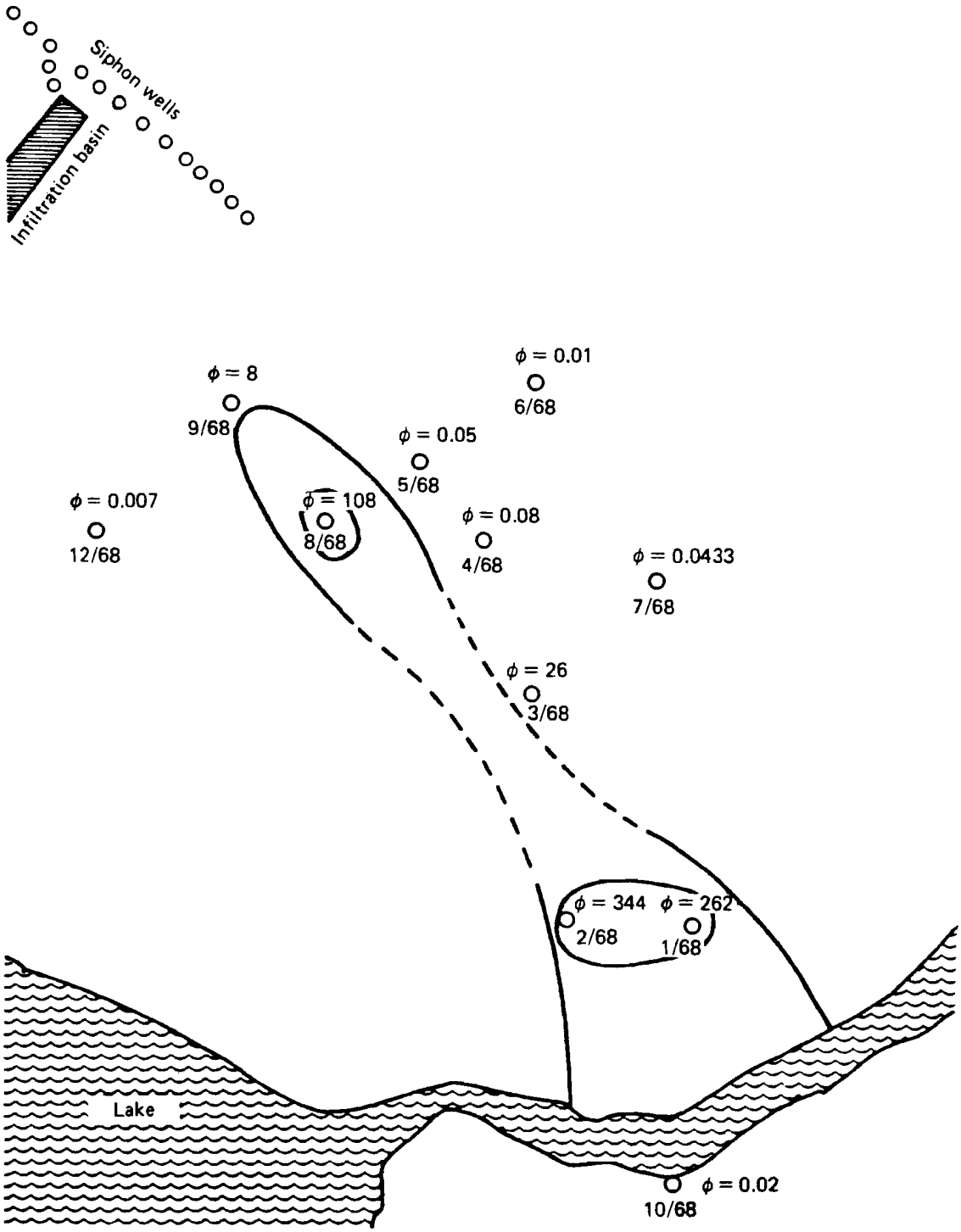

Figure 5. Observed areal extent of the contaminant plume in 1968 regarding test wells.

as will be discussed in Section 3.3.1. The transverse dispersivity β_T is related directly to longitudinal dispersivity β_L. Its magnitude is commonly much smaller than β_L ranging between $2 < \beta_L/\beta_T < 20$ (see Klotz 1982b). According to values reported previously for similar investigations (e.g. Sauty 1980, Segol and Pinder 1976, Klotz 1982b, Bruch Jr. 1970), the present study utilizes a constant ratio of longitudinal and transvers dispersivity as follows

$$\beta_L/\beta_T = 10 \quad .$$

In modeling the contaminant migration in the case study it was inherently assumed that the pollutant discharging the pore space is widely conservative; consequently sorption and possible interaction processes may be neglected, i.e.

$$\kappa = 0 \quad (R = n)$$

$$\lambda_1 = \lambda_0 = 0 \quad .$$

Furthermore, it is assumed $C' = C'' = 0$. Due to the predominance of mechanical dispersion effects the molecular diffusion is also negligible, i.e., $D_d = 0$. The migration and hydrogeologic data used in the mathematical model are summarized in Appendix B.

3.2.2. Mathematical Formulation

3.2.2.1. Discretization of Study Area

The study area Ω is appropriately discretized using biquadratic isoparametric element types. The finite element meshes employed for the fitting and predictive modeling are displayed in Figures 6 and 7. The meshes consist of 99 elements (339 node) and 100 elements (341 nodes), respectively. Inner and outer boundary contours can easily be accommodated and accurately modeled. Reasonable mesh refinements are used in areas with higher flow and/or concentration gradients to improve solution accuracy. These areas are particularly located in the plume front region (the characteristic extent of the contaminant lense for 1968 is designated in Figure 6) and near the well galleries and barrier facility.

galleries and barrier facility.

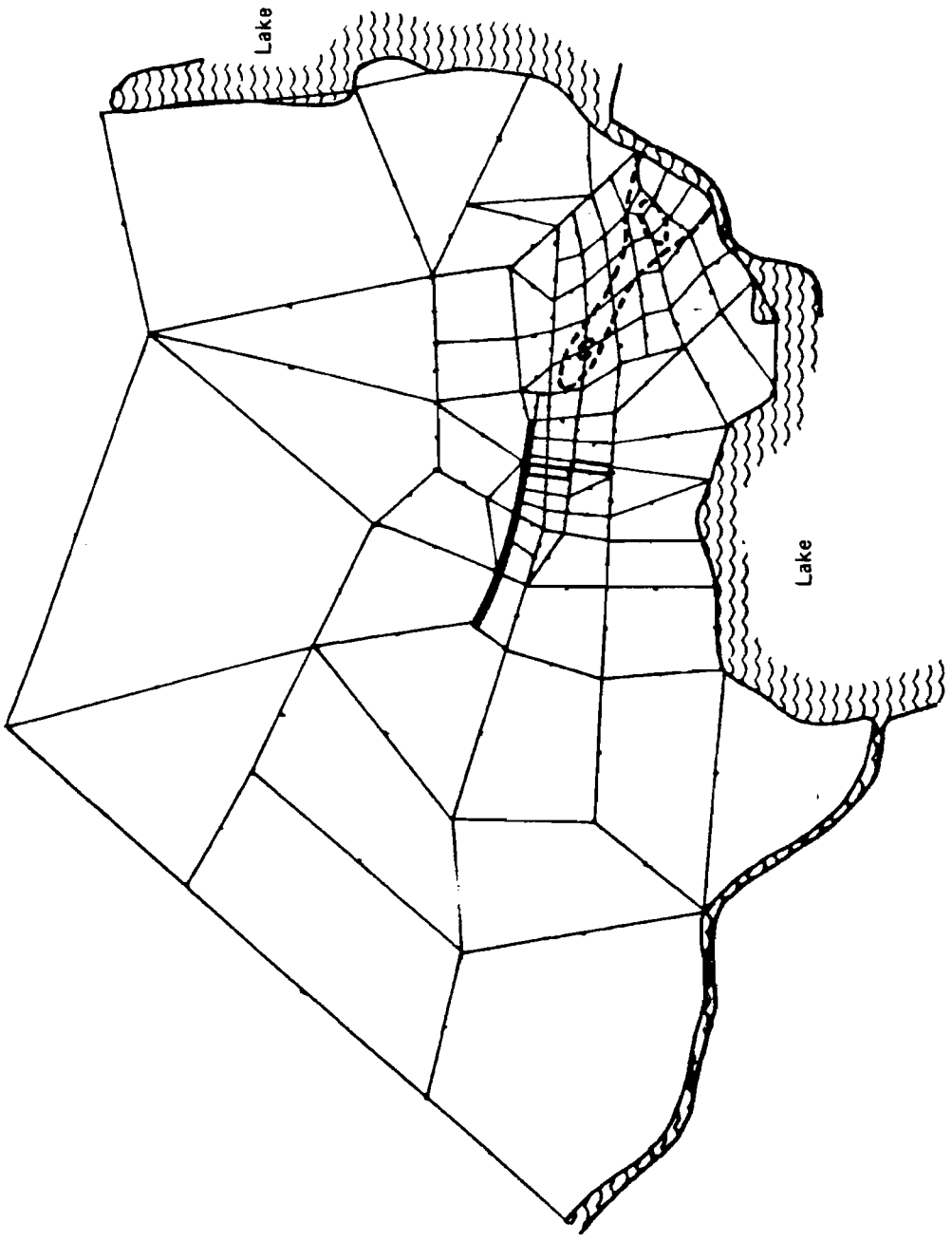

Figure 6. Finite element idealization of study area applied to epignostic modeling (99 elements, 339 nodes).

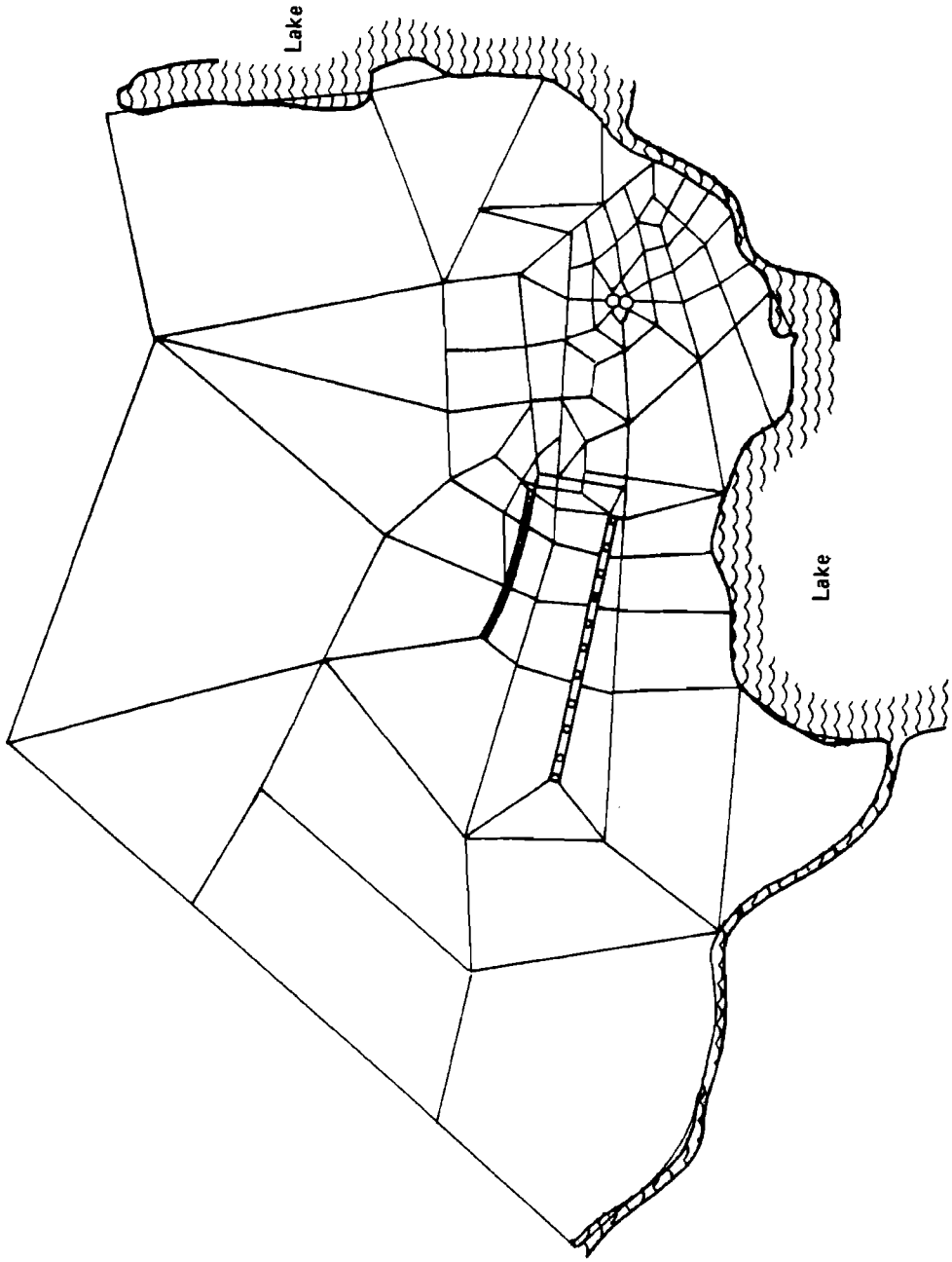

Figure 7. Finite element idealization of study area applied to prognostic modeling (110 elements, 341 nodes).

The well galleries A and B are idealized by line sinks. For the wells for interception pumping of contaminated groundwater singular well elements with circular contour are utilized. The arrangement and configuration of well elements to be used in the simulation are shown in Figure 7. Their element radius R_s amounts to 25 m.

3.2.2.2. Boundary and Initial Conditions

For inner and outer boundaries of the study area (see Figure 4), following boundary conditions are formulated which are summarized in Table 1 for the fitting period.

Table 1. Boundary conditions for $t > 0$ applied to epignostic simulation.

Boundary section of Γ		Hydraulic head h				Contaminant concentration C	
		1st kind	2nd kind	3rd kind		1st kind	2nd kind
		h_1^R [m]	q_h^R [m^2/d]	h_2^R [m]	Λ_1 [m/d]	C_1^R [mg/l]	q_c^R [$\frac{mg}{l}\frac{m}{d}$]
Outer Boundary of Study Area	ab	-	-	32.3	5.08	0.	-
	bc	-	-	32.3	5.39	0.	-
	cd	-	-	32.2	6.55	0.	-
	de	-	-	32.3	6.16	0.	-
	ef	-	-	31.9	10.63	0.	-
	fg	-	-	32.3	0.04	-	0.
	gh	-	-	32.3	3.85	-	0.
	hi	-	-	32.4	12.4	0.	-
	ijk	33.0	-	-	-	0.	-
	ka	-	0.	-	-	0.	-
Gallery A	lmnopq	-	$\frac{Q_A(t)}{L_1}$	-	-	-	0.

The kinds of boundary conditions correspond to the notation introduced in Section 2.3. The suitable boundary conditions for the prediction simulation are given in Table 2.

Table 2. Boundary conditions for $t > 0$ applied to prognostic simulation.

Boundary section of Γ		Hydraulic head h				Contaminant concentration C	
		1st kind	2nd kind	3rd kind		1st kind	2nd kind
		h_1^R [m]	q_h^R [m^2/d]	h_2^R [m]	Λ_1 [m/d]	C_1^R [mg/l]	q_c^R [$\frac{mg}{l}\frac{m}{d}$]
Outer Boundary of Study Area	ab	-	-	32.3	5.08	0.	-
	bc	-	-	32.3	5.39	0.	-
	cd	-	-	32.2	6.55	0.	-
	de	-	-	32.3	6.16	0.	-
	ef	-	-	31.9	10.63	-	0.
	fg	-	-	32.3	0.04	-	0.
	gh	-	-	32.3	3.85	-	0.
	hi	-	-	32.4	12.4	-	0.
	ijk	33.0	-	-	-	0.	
	ka	-	0.	-	-	0.	-
Gallery A	lmpq	-	$\frac{Q_A(t)}{L_2}$	-	-	-	0.
Gallery B	$\alpha\beta\gamma\delta$	-	$\frac{Q_B(t)}{L_3}$	-	-	-	0.
Barrier	rstuvwx	33.5	-	-	-	0.	-

The formulation of third-kind boundary conditions for hydraulic head h along the bank line $a-i$ allows for bottom sealing effects of the surface waters to be include.

For the north boundary, a constant water table head of 33m is prescribed in accordance with more global flow predictions. The section ka along the watershed is the only impermeable boundary with $q_h = 0$. The flow boundary conditions of second kind for the gallery A and B (Tables 1 and 2) result from transient pumping rates Q_A , Q_B according to Figure 3. Associated with their circumference lengths L_1, L_2, L_3, the line sinks will be prescribed as

L_1 = 1640m

L_2 = 1200m

L_3 = 2050m

Here, L_2 identifies the reduced L_1 length of gallery A by the omission of SWS after 1977. The Q_A- and Q_B-time relations are calculated numerically by a stepwise constant function approach with a one-year interval. For the hydraulic boundary conditions along the infiltration basin (barrier) it is more realistic and preferred here to abandon the direct estimation of the infiltration rate Q_I, and use a constant hydraulic head distribution of 33.5 m as estimated according to field measurements.

Considering the values of contaminant concentration it is possible and necessary to use homogeneous boundary conditions of first and second kind as indicated in Tables 1 and 2 for the corresponding boundary sections. In the fitting period the groundwater along the bank line a-i can be considered to be essentially uncontaminated, i.e., $C = 0$, in comparison with the plume concentration with the exception of the region f-h near the contaminant plume. According to the initial conditions to be described below, relatively high contaminant concentrations reach the surface waters. Therefore, as long as there is a groundwater inflow across that boundary section an unlimited entrance of contaminants occurs. This is always appropriate in the case of operating without a hydraulic barrier (fitting phase and intermittent operation of the barrier), in contrast to the case with an operating barrier. This can be attained via the natural boundary condition $q_c = 0$ by implying that the concentration input is purely convective here and the boundary contaminant concentration remains at the the initial condition. Such a conservative problem description is supported by the observed contaminant distribution in 1968 (compare Figure 5). On the other hand, a (too) optimistic variant would imply $C = 0$. As a compromise a boundary conditions prescription of third kind would be necessary. However, for this the transfer coefficients Λ_2 are

unknown.

For the boundary section *ijka*, in any case, the specification of uncontaminated groundwater ($C = 0$) is reasonable. Along groundwater pumping sections (outflushing contaminants) it is appropriate to use natural boundary conditions $q_c = 0$. Herewith, contaminant intrusions into the wells can sufficiently be described.

Operating with the hydraulic barrier, the groundwater in the region of the contaminant plume moves essentially in a direction towards the surface waters. The prescription of the 2nd-kind boundary conditions, ($q_c = 0$) according to Table 2, is appropriate then along the bank section $e - i$. Deviations can result if there is a reversal of the flow direction near the lake, which can only occur when there is a hypothetical four-fold increase in pumpage. This will be discussed further in Section 3.3.2.1. Under such conditions involving flow shearing one holds $C = 0$ on that boundary through which groundwater flows in. For the infiltration basin $C = 0$ is used because detailed quality data of the infiltration water are not available.

In the case of interception pumping of the contaminant plume with one or two wells (each $Q_B = 1000 m^3$) the natural boundary condition for contaminant concentration $q_c = 0$ is also applied to the singular well region. For as long as groundwater infiltrates (only for two wells as yet to be proved below), the maintaining of the condition $q_c = 0$ along the bank region fg does not allow the remediation to be complete without contaminant effluent entering the surface waters (a conservative variant). Then, the specification of $C = 0$ along *efghi* is more suitable for an "optimistic" study. Both variants will be discussed in Section 3.3.2.3.

For the transient modeling study, corresponding initial conditions for h and C are necessary. Separate sensitivity tests have proved, however, that the transient effect on the head h by the term $S\,\partial h/\partial t$ is only important over short duration transients compared with the relatively long times encountered in transient concentration travels. Therefore, it is appropriate and sufficient to run the model with (varying) steady-flow conditions. Due to the time development of pumping capacity (Figure 3) different time-stepping steady-state solutions are obtained.

The initial contaminant concentration field C in the study area is given for the observed contaminant distribution in 1968 as further indicated in Figure 5. Due to relatively sparse measured data there is the problem to quantify the contaminant concentration field and to estimate the extent of the plume. A formal transformation of concentration contour plots (Figure 5) interpolated from measured data to the finite element mesh is shown in Figure 6. For all nodal points lying within the interior of the contaminant plume, concentration values based on a simple interpolation between the measured data according to Figure 5 are assigned. On the other hand, outside this region all nodes have initially $C(x_i,0) = 0$. Finally, one yields the contaminant concentration field shown in Figure 9a for 1968 at the beginning of fitting period.

3.3. Simulation Results

3.3.1. Contamination Epignosis and Model Verification

The modeling of contaminant intrusion into gallery A especially the SWS, during the seventies serves as the model verfication period and estimation of hydrodynamic dispersion parameters. According to the given boundary conditions, the finite element method computed velocity fields as, for instance, illustrated in Figure 8 for the year 1968.

Here the average pore velocities expressed by $\hat{v}_i = \bar{q}_i / M\, n$ are displayed. The computations of the contaminant concentration fields based on a series of different dispersivities. The best reproduction of the observed contaminant intrusion into the SWS was achieved with a longitudinal dispersivity of $\beta_L = 4\ m$ and a transverse dispersivity of $\beta_T = 0.4\ m$. Higher dispersivities led to a faster and more intensive contaminant breakthrough than observed. The evolutionary migration of the contaminant plume from 1968 to 1977 is illustrated in Figure 9 by the computed concentration patterns, where contaminant iso-concentration lines are normalized by a reference concentration C_{ref}.

A comparison of the theoretical spreading with the observations is attained via the contaminant concentration pumped from the SWS (mixing concentration). It represents the integrated average of local (point)

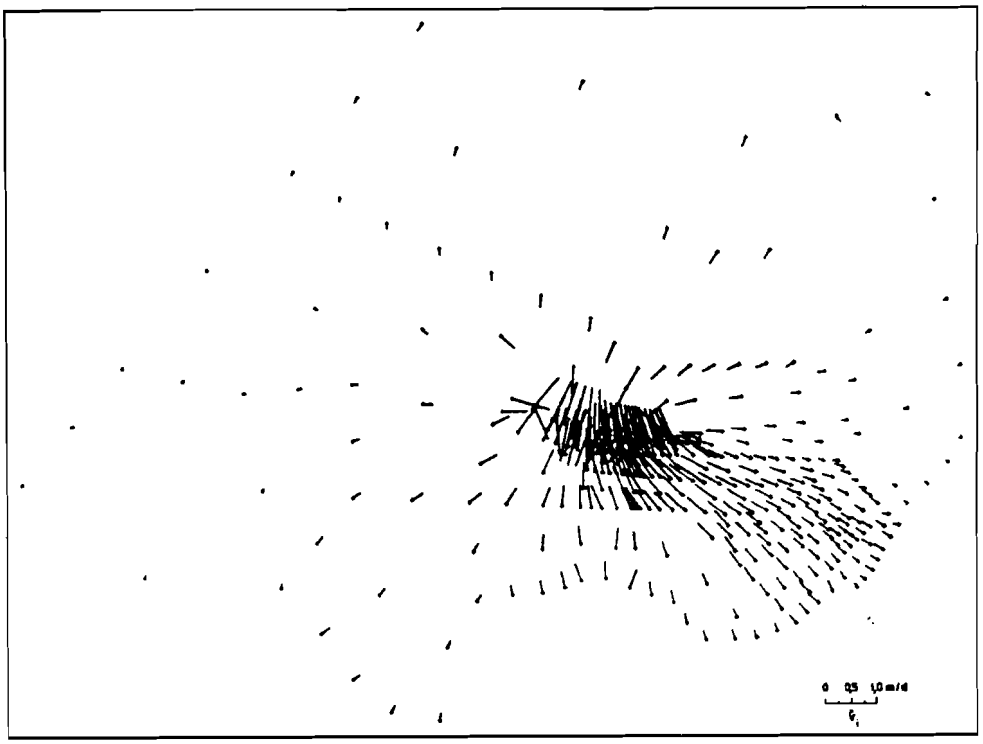

Figure 8. Computed velocity field for 1968 ($\hat{v}_i = \bar{q}_i / Mn$)

contaminant concentrations encompassing the SWS (Figure 4) as follows

$$C_H^m(t) = \frac{1}{U}\int_U C(x_{i\,|mnop}, t)\,d\Gamma \tag{21}$$

with $U = L_1 - L_2$.

The theoretical contaminant mixing water contents evaluated via equation (21) are compared in Figure 10 with the measured peak values and yearly averaged values of contaminant concentration in the SWS. Here, the computed curve is in reasonable agreement with the measured peak data: however, it is clearly above the observed yearly averaged values. As has been shown by tests, a readjustment to match with the year-mean breakthrough behaviour cannot be obtained without essential quantitative changes regarding the representative contaminant distribution at 1968 and by decreasing the

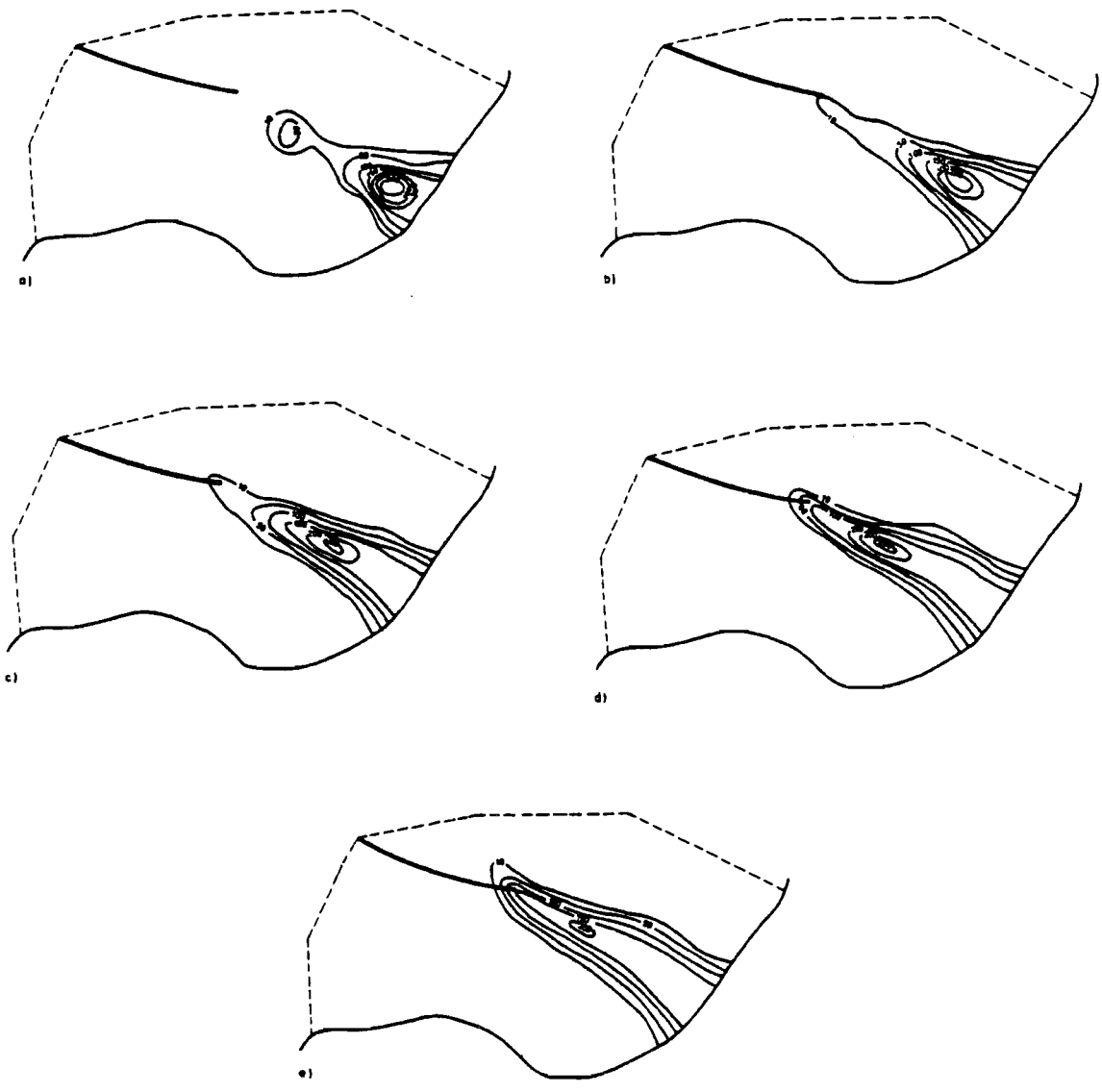

Figure 9. Computed contaminant distribution (cut-out of study area) at a) 1968 (initial field), b) 1970, c) 1972, d) 1974, e) 1977

Normalized contaminant contour levels are for C/C_{ref}, (this is valid for all following figures)

given pumping rates of gallery A. Obviously, the theoretical contaminant mixing water contents, above the observed peak data at 1970 and 1971 (Figure 10), are already in response to the exposed contaminant plume configuration having a bubble-shaped widening as stated for 1968 (compare Figures 5 and 9a). A reduction of the theoretical values in this period would require an estrangement from such initial contaminant distribution in the leading edge. To compromise in face of those experimental discrepancies, the computed theoretical behaviour of the contaminant breakthrough into SWS can be valued to be sufficiently representative. It characterizes quantitatively a conservative model solution.

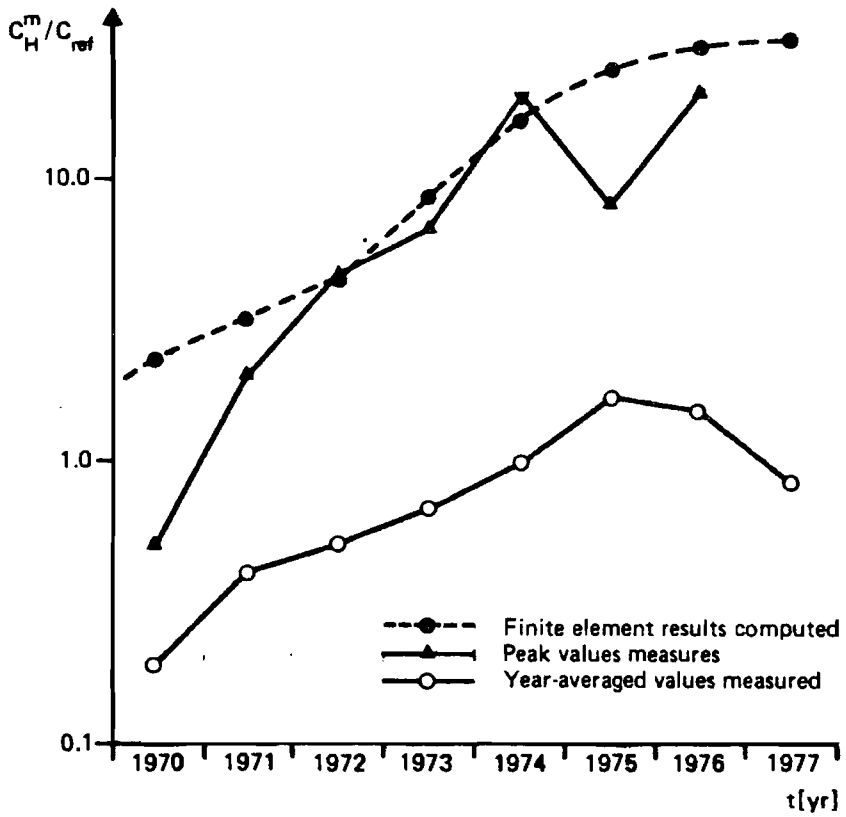

Figure 10. Computed results versus experimental history of contaminant contents in pumped mixing water of SWS during the epignosis period from 1970 to 1977.

3.3.2. Prognisis for Contaminant Intercepting and Aquifer Remediation

3.3.2.1. Hydraulic Barrier by Recharge

After beginning the operation of the hydraulic barrier and gallery B in the period since 1978, a significant alteration of hydrodynamic regime appears in the study area. This is clearly seen by the computed velocity field plotted in Figure 11 for the years $t \geq 1983$ concerning the mean pore components $\hat{v}_i$. The computations based on the pumping rates are indicated in Figure 3.

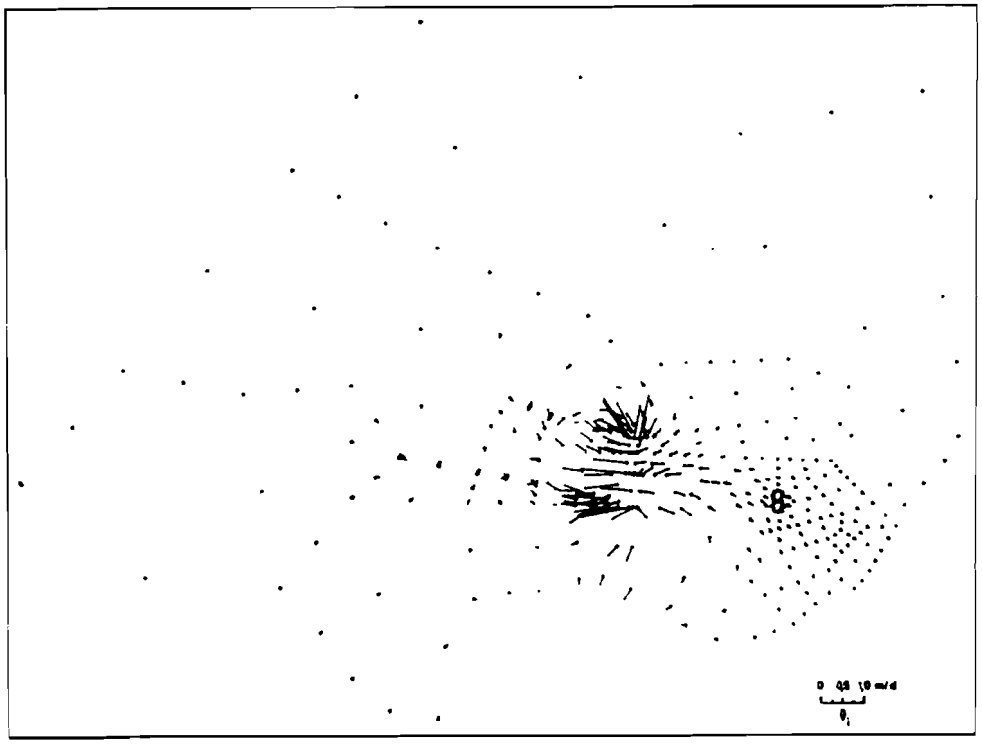

Figure 11. Computed velocity field for $t \geq 1983$ ($\hat{v}_i = \bar{q}_i / Mn$).

The velocity field reveals a short-circuit groundwater flow between basin and supply wells with relatively high velocities, caused by infiltration, and the movement towards surface waters in the contaminant plume zone, which however is relatively small. Low velocity zones occur (among others) easterly in the study area near the lake. It is of further interest to note the flow

removing zone north of infiltration basin in the influence of gallery B.

The effects of the hydraulic barrier on the contaminant plume movement are demonstrated by the computed concentration patterns plotted in Figures 12a-e for several years. For these predictions the pumping and infiltration conditions from Figure 3 are assumed to be valid in future. Concerning the initial conditions the concentration distribution computed for 1977 (Figure 9e) is used. The hydraulic barrier acts relatively quickly on the near-well regions. The concentration field obtained for 1978 (Figure 12a) depicts how the leading edge of the contaminant plume is "cut off", due to northerly flow removing, and migrates towards gallery A (now reduced by the SWS). However, no impacts on the greater part of the contaminant plume can be seen at this time. After two years, at 1980 (Figure 12b) the response to the action of hydraulic barrier is already evident. Due to the groundwater moving completely towards the surface waters, the contaminant plume draws gradually backward. This flushing back is associated with north-east turning of the contaminant plume around its centre.

The process becomes progressively slower the farther the plume drifts away from the barrier. The predicted contaminant concentrations for the year 1986 shown in Figure 12c depict these effects. For the year 1993 Figure 12d reveals distinctly the reduced contaminants effluent level entering the surface waters. A later time shows a further progressive stage of the contaminant interception as displayed in Figure 12e for the year 2010. The late phase is characterized by a long tailing effect of contaminant flush entering the surface waters. By 2025 the contaminant plume has 'bled out' completely. It should be recalled that this is only valid for the assumption made regarding free mobility of phenols in the sediment (compare Section 3.2.1.2).

The predicted iso-concentration patterns indicate that the contaminant plume revolves completely towards the surface waters under the given supply and recharge conditions (Figure 3). The core of the plume immediately drifts slowly in north-eastern direction.

The measure of contaminant effluent entering the surface waters is obtained by an integral evaluation of contaminant concentration and groundwater velocities along the bank line fgh (section designated in Figure 4). The contaminant effluent P_A in $[t/yr]$ is given by

$$P_A(t) = \int_{\Gamma_{fgh}} \bar{V}(x_{i|fgh}, t)\, C(x_{i|fgh}, t)\, d\Gamma \qquad (22)$$

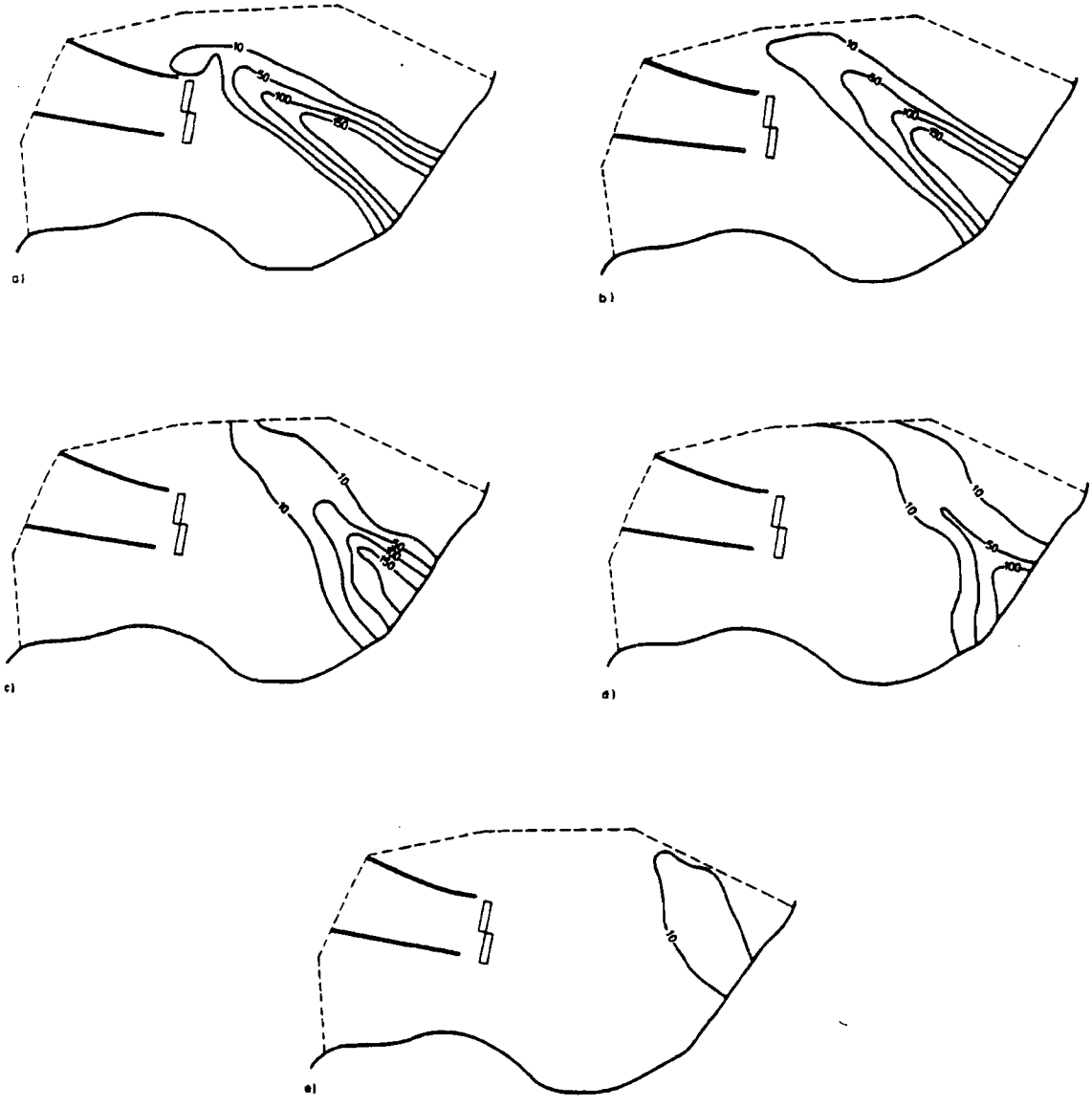

Figure 12. Computed contaminant distribution (cut-out of study area) under permanent operating of phenol barrier for prognosis period in a) 1978, b) 1980, c) 1986, d) 1993, e) 2010.

representing the convective mass flux. The dispersive contribution $\int q_c \, d\Gamma$ is enforced to be zero due to the natural boundary condition. After computing velocity and concentration distributions we get the following behaviour of transient contaminant effluent entering the surface waters as depicted in Figure 13.

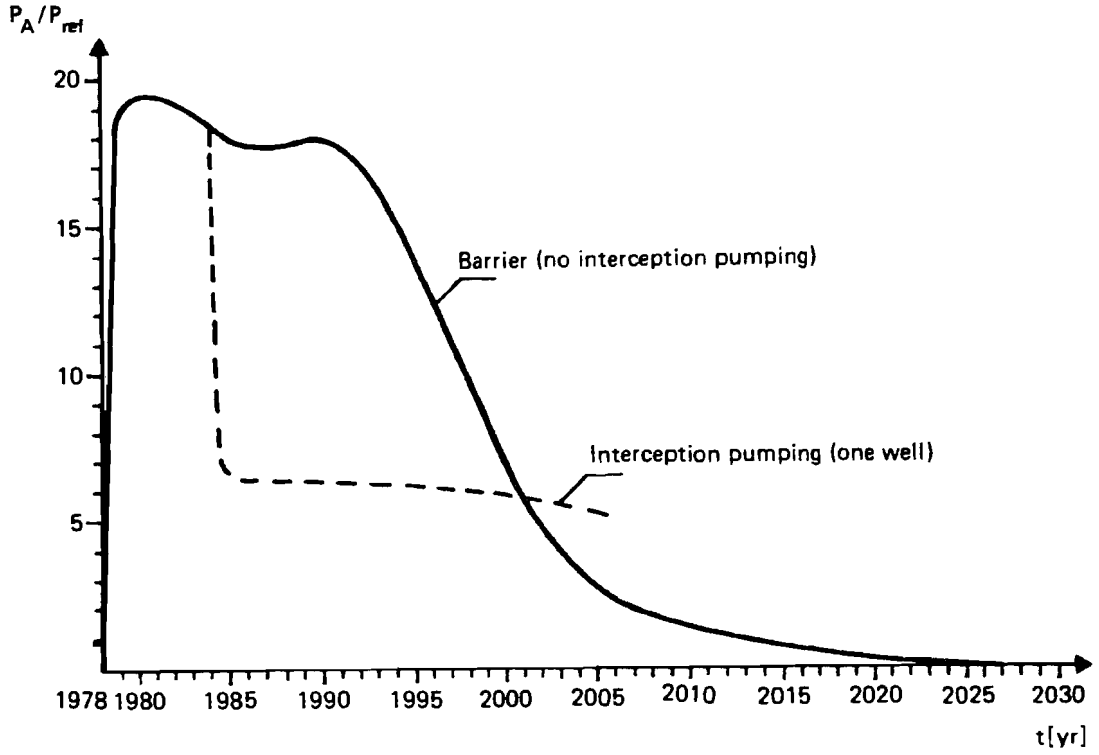

Figure 13. Computed history of normalized contaminant effluent P_A / P_{ref} entering the surface waters under permanent operating of hydraulic barrier.

A distinct decline of effluent behaviour can be seen for the nineties. Tailing effects are typical in later years. The process requires altogether approximately 50 years. The entire effluent contaminant masses are taken to be contents in the study area as simulated up to 1977 according to the initial and boundary conditions. To make clear additionally the hydrodynamic influence on the process, a comparison with a hypothetical case of a four-fold increase in pumpage of supply station (as originally planned) is studied. The resulting concentration fields are computed and are illustrated in Figures 14a-c for

three characteristic years. The vital point is that, due to the higher pumping capacities, now the entire contaminant plume is not any more governed by a global eastward groundwater movement. Here, a flow shearing in the north and north-east occurs, where opposing flows and velocity-reduced zones adjoin. The consequences for the contaminant distribution, resulting from this situation are observable in Figure 14a for the year 1988.

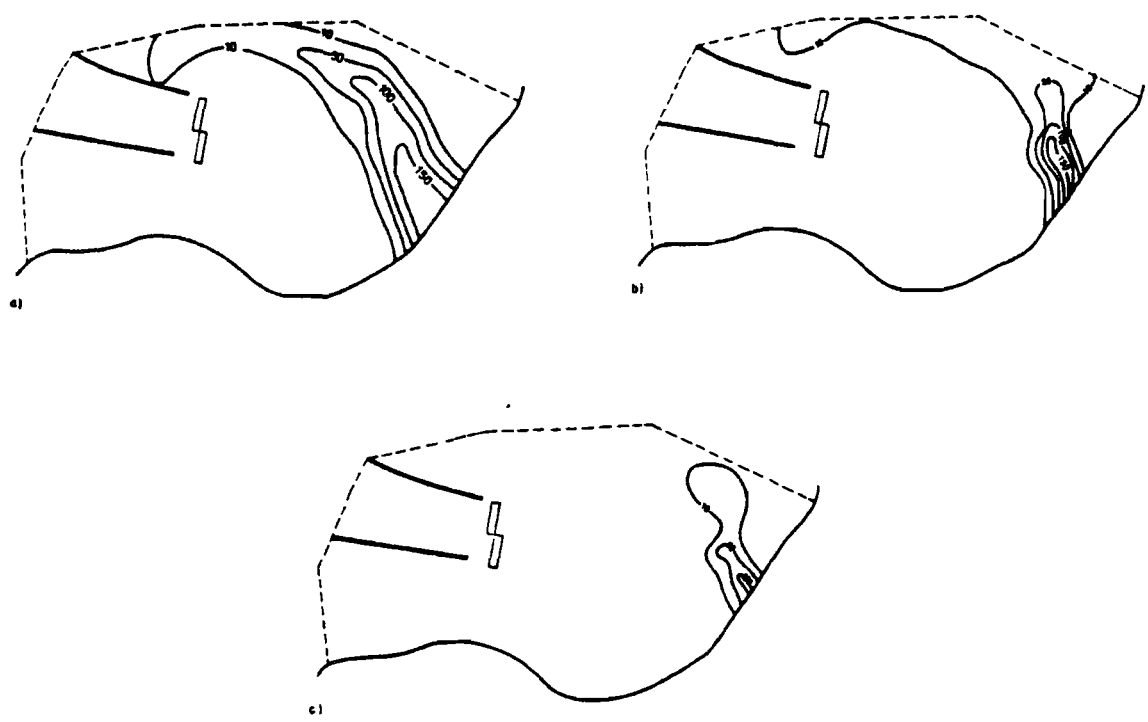

Figure 14. Hypothetical movement of contaminant plume at four-times higher water supply under barrier operating (cut-out of study area) for a) 1988, b) 2027, c) 2060.

Now, the contaminant barrier has proved to be only partially effective and is not completely 'tight'. Due to the northern flow, contaminants further intrude into the gallery A over a long period. Even at late times, as shown in Figure 14b for the year 2027, a diluted zone reaches up to the gallery A. Very slowly, only in the course of the continuous hydrodynamic 'drag' action on the plume, is the contaminant diluted and flushed out. A developed stage is displayed in Figure 14c for the year 2060. Therefore, the contaminant effluent

entering the surface waters is essentially lower than the comparable model case and amounts only to 12% as a maximum. A comparison with Figure 13 reveals a descending characteristic over a very long period. Altogether the process covers about 130 years!

3.3.2.2. Intermittent Operation of Hydraulic Barrier

With a view to effectiveness, and considering that it is a feasible option, intermittent operating states of the infiltration basin will now be discussed.

The set of contaminant distributions illustrated in Figures 15a-e reveals the effects of intermittent operation. It refers to the hypothetical case that the hydraulic barrier has ceased since 1982. The resulting return motion of contaminants in the following years towards the yielding galleries is depicted in Figures 15a-c. After 5 years (1987, as evidenced in Figure 15b) higher contaminations result again, especially of gallery *A*. Again 6 years later (1993, as evidenced in Figure 15c) a developed stage of contaminant intrusion into the wells is already pronounced. After the hydraulic barrier is again put into operation beginning with 1993 the contaminant concentrations in the study area change as illustrated in Figure 15d for 1995 and in Figure 15e for 2003. Obviously, the contaminant plume can effectively be driven back. However, the plume spreads increasingly as a result of hydrodynamic dispersion.

To identify and describe the risk and effectiveness of intermittent operating to the wells the mean contaminant content $C_B^m[mg/l]$ of the first three wells of the leading section of gallery A will be further considered. Figure 16 displays several variants of intermittent operating with their consequences on the contaminant content C_B^m (normalized by the reference concentration C_{ref}) in these wells. The phase of interception designated by "1" describes the passing contaminant increase due to the 'cutting off' of the contaminant plume during the operation of the barrier in 1978. The interruption of the hydraulic barrier in 1982 (phase marked with "4" in Figure 16) leads to a significant increase of contaminant contents in the wells over time. The concentration patterns plotted in Figures 15a-c refer to this phase. The variants designated by the numbers "2" and "3" in Figure 16 demonstrate different times of restarting the hydraulic barrier. In both cases the occurred contamination is quickly reduced to zero, athough the solution is based on different initial levels.

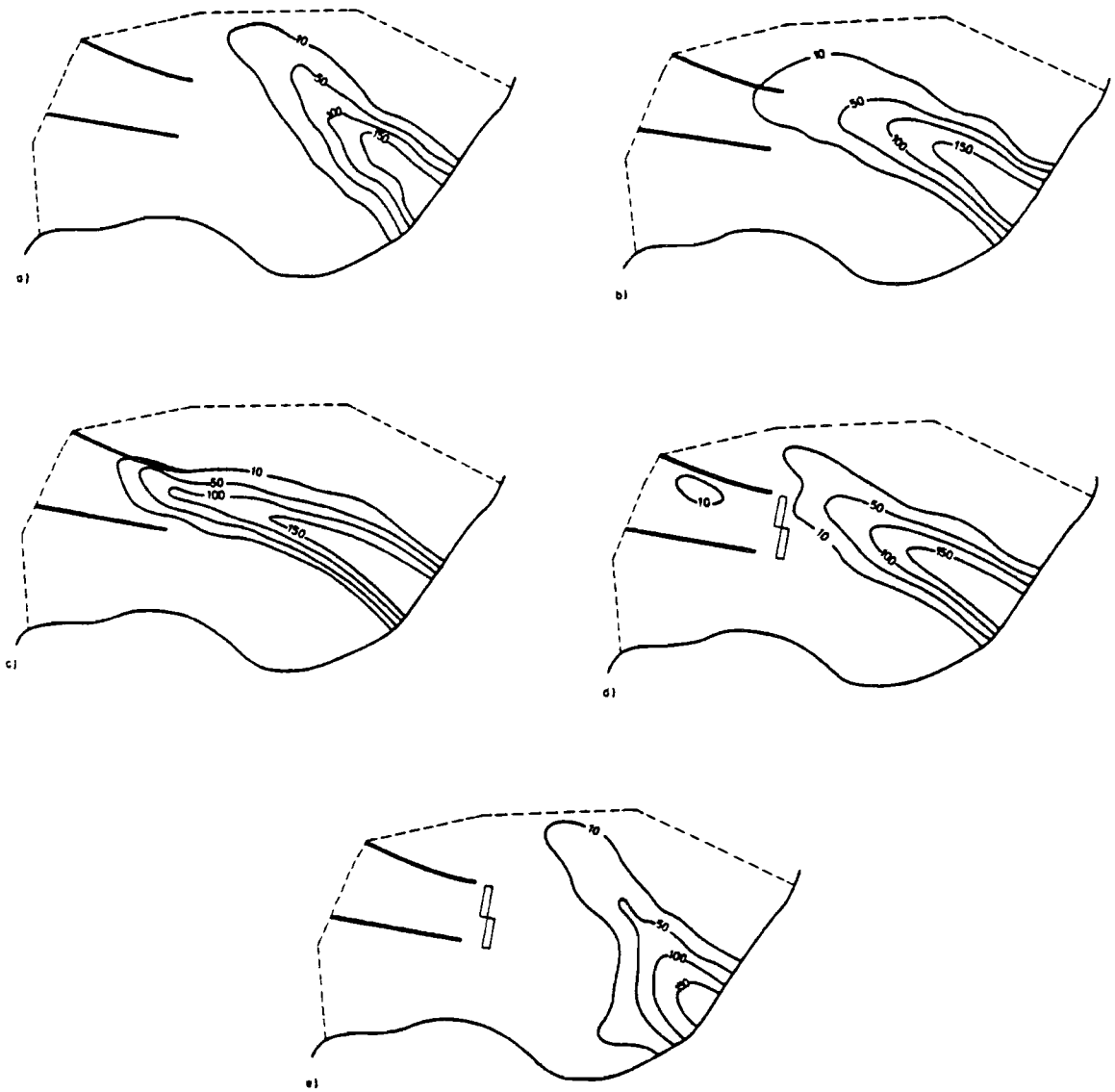

Figure 15. Movement of contaminant plume for intermittent operating of hydraulic barrier (cut-out of study area) at a) 1983, b) 1987, c) 1993, without barrier (since 1982), d) 1995, e) 2003 with barrier (since 1993).

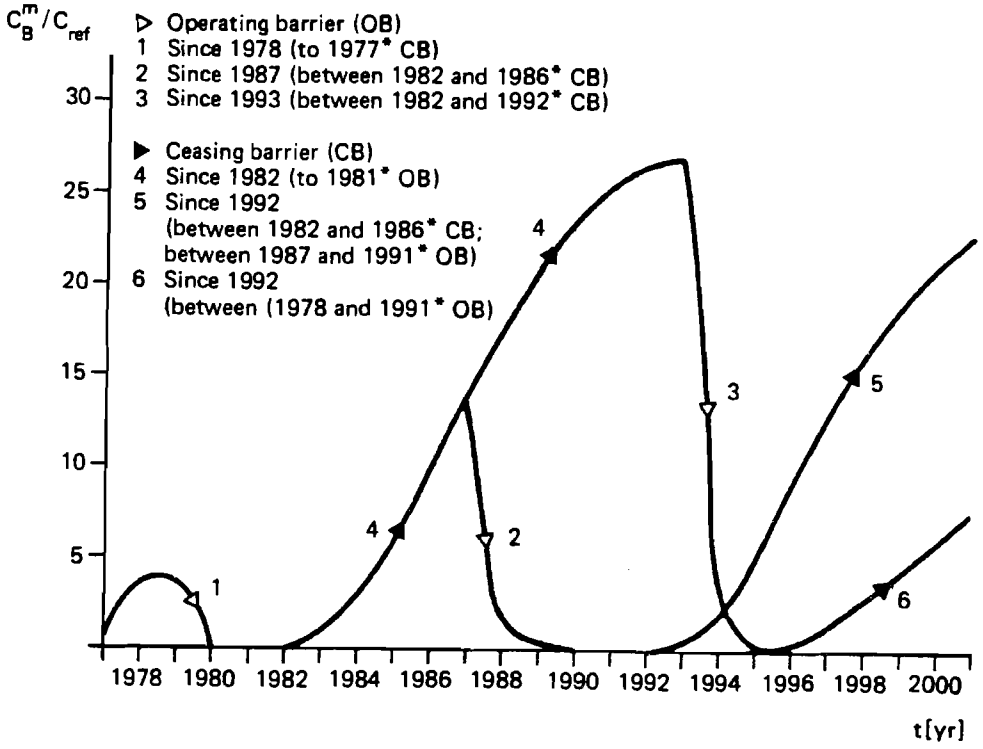

Figure 16. Predicted increase and descent of contaminant content in leading wells of gallery A for variants of intermittent operating the hydraulic barrier (* up to the end of the year concerned).

The interception phase identified by mark "3" corresponds to the concentration distribution shown in Figures 15d, e. If an interval between restarting and ceasing the hydraulic barrier is chosen to be five years, one obtains the characteristic as indicated in Figure 16 by code numbering 1 - 4 - 2 - 5. The measure of re-increasing the contaminant contents C_B^m at ceasing the barrier is nearly equal in the phases "4" and "5" having a time difference of 10 years. After 3 years C_B^m exceeds in each case the level of 5 for instance.

It is obvious to use a non-equidistance in intermittent operating where the interception phase should enclose a sufficiently longer period. Therefore, the contaminant plume can be driven farther away and flushed out in the surface waters to a greater extent. A following phase without hydraulic barrier can profit by this intermittent operaing policy due to necessarily longer times

for removing and the dilution effects that have occurred in the meantime. For instance, considering the case marked with "6" in Figure 16, a significantly retarded re-increase of well contamination C_B^m is observable when the hydraulic barrier ceases only from 1992. The mode of operating the hydraulic barrier corresponds to code numbering 1-6 in Figure 16, i.e., the characteristic of moderate re-increase (designated by mark "6") is a result of 14 years barrier operating.

It can be concluded that intermittent operating is only reasonable when the interception phase dominates temporarily. However, due to the oscillation of the contaminant plume between the infiltration basin and lake the plume spreads increasingly, albeit accompanied by dilution. This is opposed to an effective decontamination of aquifer.

3.3.2.3. Interception Pumping of Contaminant Plume

To clean the aquifer, it is possible to pump contaminated groundwater from the area and to transport it to a treatment plant. The effectiveness and effect of such an arrangement is discussed below.

Two variants of remedial pumping the contaminant plume will be further examined:

(a) Using one well with Q_B = 1000m^3/day

(b) Using two wells with total 2000m^3/day (each Q_B = 1000m^3/day)

For their location in the area a possibly plume-central position is selected as indicated in Figure 7 by the singular well elements. For variant (a), the case with only one well, the southernmost location will be come into question. Firstly, it is presumed that the hydraulic barrier operates continuously. Without pumping, the entire contaminant plume would consequently be flushed out into the surface waters, see Section 3.3.2.1. On the other hand, in the case of interception pumping the amount of contaminant effluent entering the surface waters is either reduced partly or totally. According to the computed flow patterns, it can be seen that when applying only one well with a capacity of 1000m^3/day the pumping is not strong enough to capture all of the contamination. Along the entire bank region the contaminant plume is now as ever convected eastward to surface waters; however, the groundwater movement is significantly reduced. Figure 13 indicates how the contaminant effluent $P_A(t)$ entering the surface waters (according to equation (22))

responds concerning the hypothetical case that pumping begins in 1984. Obviously, further on there is contaminant flushing out, although the maximum level is reduced by more than half. However, this diminished level of P_A burdens the surface waters over a long period. The poor decrease for P_A reaches very far up to the next millennium when using one well.

Resorting to two wells the entire contaminant plume can convectively be governed. Now, along the bank line fg there are inward-directed flow conditions (infiltration). Consequently, the contaminant effluent entering the surface waters vanishes: $P_A(t) = 0$. The total contaminant masses of the contaminant plume can therefore be captured in both wells.

Due to finding infiltration along the bank line fg, variants of boundary conditions for contaminant concentration C are to be discussed, as has already been pointed out in Section 3.2.2.2. The specification of $C = C_1^R = 0$ along the bank line implies an uncontaminated inflow and therefore the entire aquifer can be pumped free of contaminants (optimistic variant). This process is indicated in Figure 17 by the predicted concentration distribution for the years 1985, 1995 and 2015 provided the pumping starts simultaneously with two wells at 1984. As a counterpart to this case, illustrated in Figure 17, the conservative variant of boundary condition $q_c = q_c^R = 0$ along the bank line fg does not allow the aquifer to decontaminate because boundary contaminant concentrations drop to zero. Accordingly, the region between bank section fg and the wells remains contaminated (steady state).

It is of practical interest to predict the mixing concentration of water pumped by the wells which are utilized for interception. For a well (a) the mixing concentration is given by

$$C_B^a(t) = \frac{1}{U}\int_U C(x_u,t)\,d\Gamma \tag{23}$$

with $U = 2\pi R_s$, where x_u represents the well circumference coordinates (circular contour). Using two wells (a) and (b) the mixing concentration of pumped water can be computed by

$$C_B^m(t) = \frac{C_B^a \cdot Q_B^a + C_B^b \cdot Q_B^b}{Q_B^a + Q_B^b} \quad , \tag{24}$$

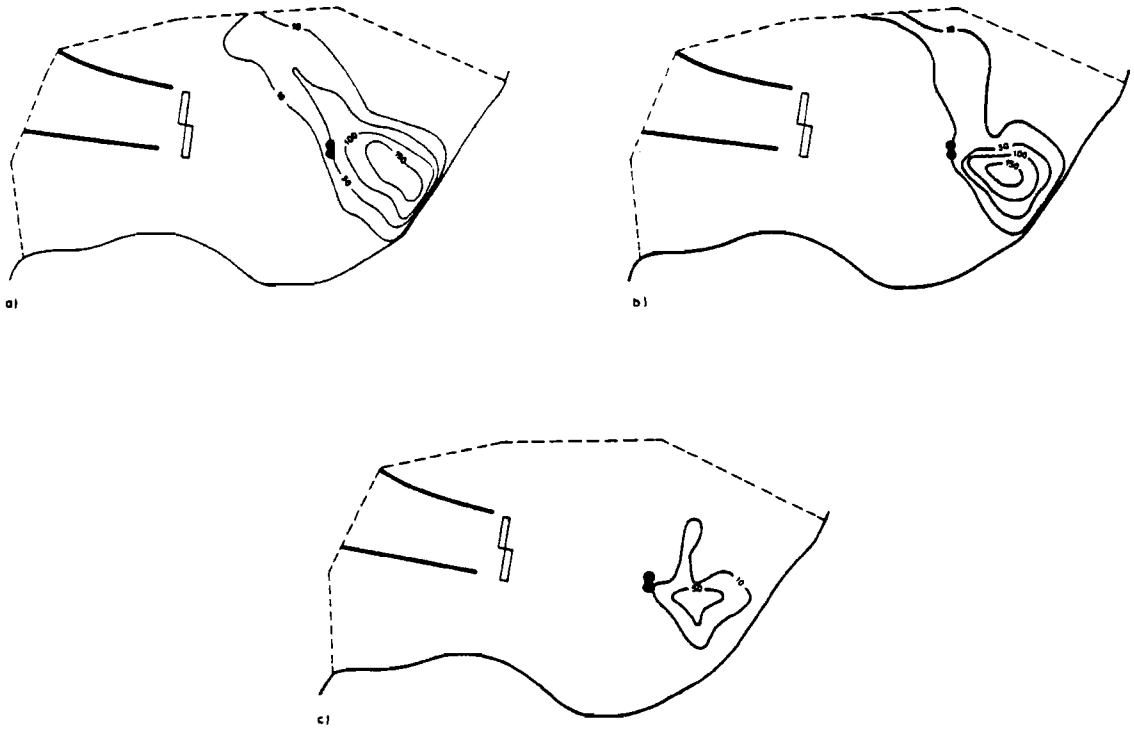

Figure 17. Predicted degradation of contaminant plume by applying two wells (total 2000m^3/day) starting 1984, under unceasing operating the hydraulic barrier, and with uncontaminated infiltrate ($C_1^R = 0$ along *efghi*); a) 1985, b) 1995, c) 2015

where Q_B^a, Q_B^b are the pumping rates of wells and C_B^b corresponds to the well mixing concentration of well (b) analogous to equation (23). In case of only one well there is $C_B^m = C_B^a$, because $Q_B^b = 0$. Otherwise, two wells with constant capacities $Q_B^a = Q_B^b = Q_B$ yield $C_B^m = (C_B^a + C_B^b)/2$.

The numerical evaluation of mixing concentrations C_B^m based on equations (23) and (24) from the computed contaminant distributions leads to the following curves for the interesting variants as shown in Figure 18. Utilizing only one well it can be seen that the well-influenced region is pumped free after about 25 years. Differences between the variants of boundary conditions ($C_1^R = 0$; $q_c^R = 0$) do not appear here. Maximum values occur after 2 years computed from the beginning of pumping in 1984. The passing increase of C_B^m-curve arises from travelling of the contaminant plume towards the well.

However, for one well the contaminant plume cannot be captured by interception pumping. Defining the contaminant effluent entering the pumped well as

$$P_B(t) = Q_B^a \cdot C_B^a + Q_B^b \cdot C_B^b \qquad (25)$$

a comparison reveals that, using only one well, fewer than 20% of contaminant masses over a period of about 25 years are pumped, more than 80% bypassing the well enters the surface waters.

Unlike this, two wells allow the entire contaminant plume to be captured. However, a rather considerable time is necessary. Passing peak values amounting to about double the size of only one well descend over a long period of about 50 years (compare Figure 18). The consequences of the different boundary conditions at the bank are seen only after a long period. As evidenced in Figure 18, for the case of two wells the mixing concentration tends to a constant value only after the year 2000, while C_B^m for $C_1^R = 0$ decreases slowly to zero.

Returning to Figure 17 for a further discussion it is evident that the long pumping times needed, which are associated with distinct tailing characteristic of well mixing concentration C_B^m (see Figure 18), must be expected in response to the hydrodynamic action arising from the hydraulic barrier itself. As a typical exterior feature for this it is indicated by a 'hanging' of contaminant plume at the well leeside (Figures 17a-c). The predicted transient concentration development, after simultaneous ceasing of the hydraulic barrier during interception pumping with two wells (involving $C_1^R = 0$), is shown in Figures 19a-c. Obviously, without the hydraulic barrier the interception pumping procedure can be carried out in a much shorter time. However, the entire contaminant plume is not governable leading to re-contaminations especially in the gallery A (compare Figures 19b,c). The predicted well mixing concentration C_B^m for this case without hydraulic barrier is further described in Figure 18. The pumping here needs only 15 years. Peak values are more than double the contaminant concentrations of a comparable case with the barrier operating. However, only about 60% of contaminant masses enters the intercepting wells. The rest migrates to the yielding galleries, especially the gallery A. In Figure 18 the temporal increase and later descent of mixing concentration in wells leading the gallery A are also indicated. Its maximum contamination occurs after about 10 years since the beginning of the interception

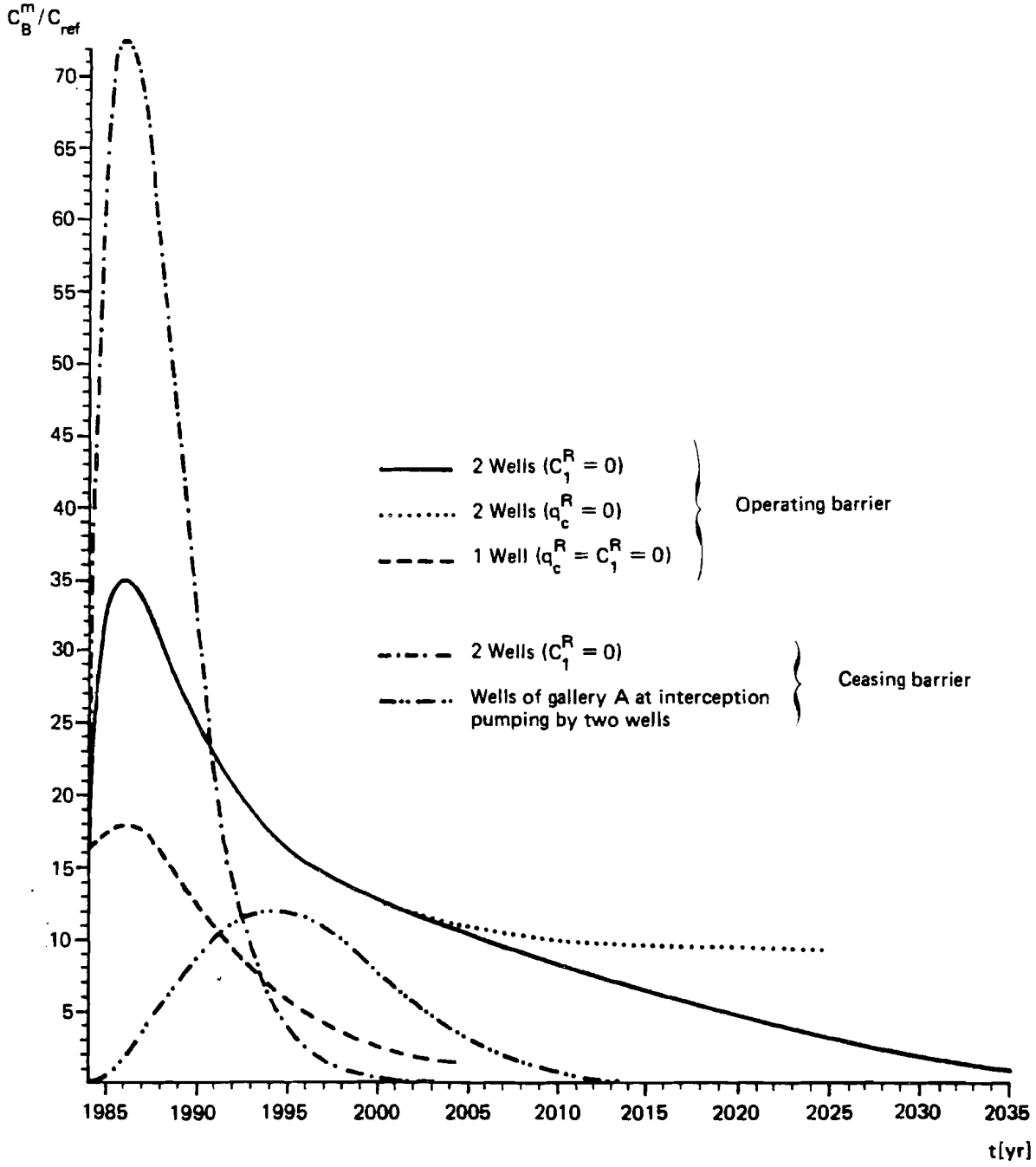

Figure 18. Transient development of normalized well mixing concentration C_B^m / C_{ref} predicted involving interception pumping the contaminant plume with and without barrier operation.

pumping and simultaneous shut-down of the hydraulic barrier. The entire duration for re-contaminating the leading wells of gallery *A* is more than 25 years.

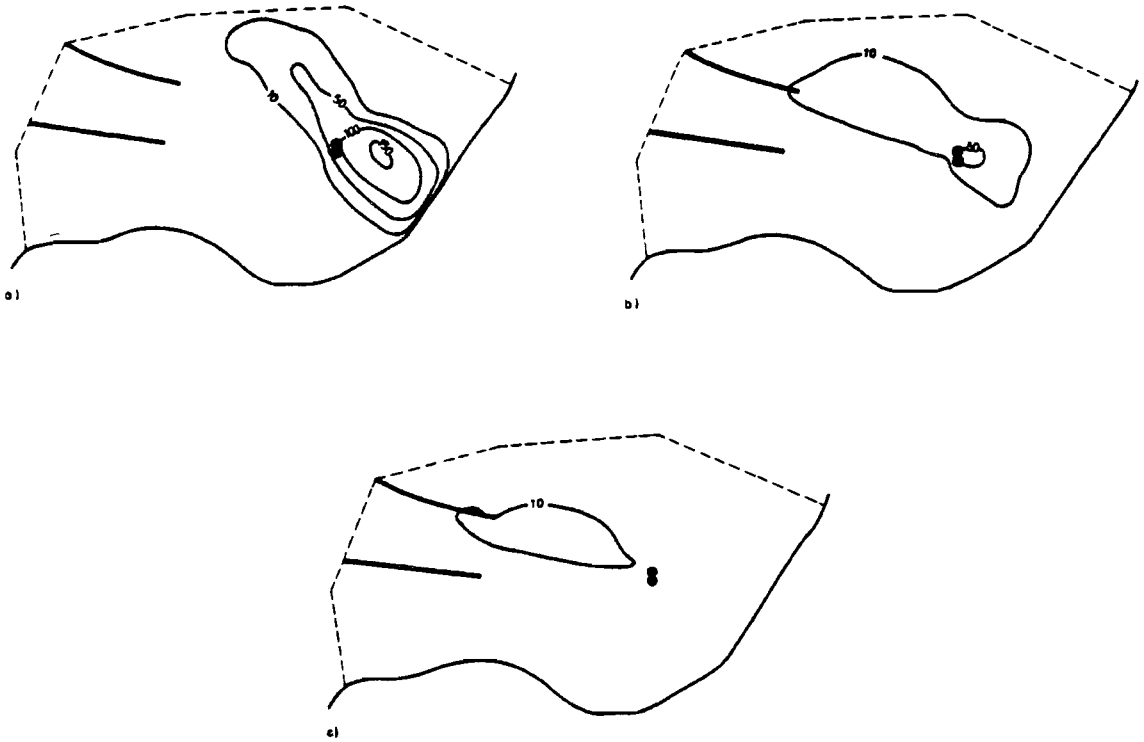

Figure 19. Predicted degradation of contaminant plume by applying two wells (total 2000m^3/day) with the beginning of the year 1984, under ceasing the hydraulic barrier, and with uncontaminated infiltrate ($C_1^R = 0$ along efghi); a) 1985, b) 1990, c) 1995.

3.4. Conclusions

The finite element method has proved to be a helpful tool in modeling the complicated flow and transport processes of the present contaminant plume. The developed mathematical model based on a horizontal process description was verified by the observed historical contaminant breakthrough characteristic in the SWS of the gallery A (model fitting period from 1968 to 1977). A reasonable match of the theoretical behaviour with field data was achieved for dispersivities of $\beta_L = 4m$ and $\beta_T = 0.4m$ (Figure 10). The measured

contaminant distribution at 1968 was used to be the initial field in modeling (Figure 5).

The numerical field study was based on the finite element configurations as exhibited in Figures 6 and 7. The used time steps Δt ranged from one to maximum 12 months. Both Crank-Nicholson, and (in case of need) fully implicit time marching schemes were run.

The transport model was used to study the action and effectiveness of current and intended contaminant interception and overall remedial strategies for water resource of the supply station considered. The obtained prognostic results allow practical conclusions to be drawn:

- The perfection of the hydralic barrier by recharge depends strongly on the pumping capacity of the supply station, especially of gallery *A*. With the current reduced level of supply a complete interception of contaminant plume is possible, provided infiltration recharge remains at a given level. Then contaminant removing and re-intrusion do not exist (Figure 12).
- An increase of water supply capacity, without appropriate expansion of infiltration, significantly enlarges the risk of intruding contaminated groundwater, especially into the gallery *A* due to flow removing and shearing as for instance proved with a hypothetically four-times higher water supply (Figure 14).
- On principle, the overall remediation of aquifer needs very long times. At continuous operation of the hydraulic barrier and under maintenance of the current water supply capacity (Figure 3) about 50 years elapses till the contaminant plume is completely driven away and flushed out into the surface waters. Using higher pumping capacity the process is further retarded. In the case of four-fold increase in supply, about 130 years are expected to be necessary (Figures 12 and 14).
- The contaminant effluent entering the surface waters was predicted by the numerical model. A distinct descent of effluent behaviour is forecasted for the nineties. Long tailing effects are shown in later years (Figure 13).

- The intermittent operation of the hydraulic barrier has proved to be effective and profitable only under restrictive conditions. An intermediate and short-term ceasing of the barrier is allowable. However, long-term ceasing in range of months or years leads already quickly to contamination problems in water supply if it was not preceded by a very long interception (Figure 16).
- In case of remedial pumping of the contaminant plume by one or two wells with each having a capacity of 1000m^3/day, relatively long decontamination times, in order of decades, are also necessaary. Here it is worth noting that the more reliable the measure the longer the remedial process.
- Applying only one well for interception pumping only about 20% of contaminant effluent enters the surface waters. However, the contaminant load per time unit is reduced by more than half compared with the case without interception pumping. On the other hand, the influence of contamination on the surface waters enlarges upon a much longer period, but on reduced level (Figure 13).
- Using two wells for interception pumping, the contaminant masses can be totally captured. Then influences on surface waters do not any more occur. However, the transient contaminant load in the wells and necessary pumping times depend strongly on how and in which intensity the hydraulic barrier co-operates. With the hydraulic barrier, about 50 years are necessary to decontaminate the aquifer. At simultaneous ceasing the hydraulic barrier the interception pumping process duration reduces to 15 years, where the peak values of well mixing concentration increase. However, the entire contaminant plume is no longer governable and only 60% of the contaminants can be pumped out. The remaining contaminant masses migrate to the gallery A and cause there contaminations over a period of about 25 years (Figure 18).
- For sufficiently high well discharge (here 2000m^3/day), the interception pumping of the contaminant plume appears suitable to decontaminate the water resource of supply station and to protect the surface waters from further contaminant intrusions. To reduce the necessarily long operation times for pumping the infiltration capacity of the hydraulic barrier may be diminished. However, it increases the risk of re-contaminating the wells of the supply station. A longer complete ceasing

of hydraulic barrier should generally be avoided.

4. Research Needs

The case study illustrates the aptitude of finite-element simulation techniques for the forecast of responses of polluted aquifers to remediation measures. Steady-state as well as transient mass transport problems can be solved. Furthermore, different physico-chemical properties of the contaminants can be considered. In our study, the contaminant was supposed to be a conservative tracer. This assumption was made because of the lack of knowledge about parameters of sorption as well as chemical or biochemical degradation in the underground. Consequently, the computed results might be too pessimistic. In the future, the effect of these processes should be taken into account. Undoubtedly, they may change drastically the choice of remediation technologies. For instance, in our study the intermittent operation of the hydraulic barrier was proved to be not very effective. The contaminant plume spreads increasingly. But just this effect could be of interest due to the increase of the reaction space for chemical or biochemical degradation.

The study makes the long-term character of aquifer remediation measures evident. Consequently, these measures are becoming extremely expensive. A careful examination and choice of remediation techniques therefore is of great importance. In making this choice, besides the aquifer remediation itself, further goals or objectives as the satisfying of water demand, the minimizing of surface water pollution, the minimizing of treatment costs, etc., have to be taken into account. Thereby different interest groups or decision makers are involved.

In general, policies for the remediation of polluted aquifers have to be embedded into complex regional water (environmental) policies. To do this convincingly, the complicated simulation models, and their results have to be integrated into more complex decision support model systems. The most promising way would be the simplification of these models. For the simplification of nonlinear mass transport problems as the remediation of aquifers generally are characterised, appropriate methods do not yet exist. Groundwater quality management models that include nonlinearities represent a key area for research (Gorelick 1983).

APPENDICES

Appendix A: Finite Element Approximation

Using (in the present case) a biquadratic interpolation over each finite element e of the unknown functions h, q_i, C according to equations (14) and the weighting function $N = N(x_i)$ with the finite element assembly process as

$$\int \int_{\Omega} ( ) \, d\Omega = \sum_{e} \int \int_{\Omega^e} ( ) \, d\Omega \tag{A1}$$

$$\int_{\Gamma} ( ) \, d\Gamma = \sum_{e} \int_{\Gamma^e} ( ) \, d\Gamma \tag{A2.}$$

the finite element model equations (15) and (16) lead to the matrix formulations as

$$\mathbf{S} \cdot \frac{d\mathbf{H}}{dt} + \mathbf{T} \cdot \mathbf{H} = \mathbf{Y} \tag{A3}$$

$$\mathbf{R} \cdot \frac{d\mathbf{C}}{dt} + (\mathbf{K} + \mathbf{D} + \mathbf{Q}) \cdot \mathbf{C} = \mathbf{Z} \tag{A4}$$

where **S**, **T**, **R**, **K**, **D** and **Q** are $(m-d) \times (m-d)$ dimensional matrices (d designates the number of passive nodes containing Dirichlet-type boundary conditions) of banded structure; **H**, **C**, $d\mathbf{H}/dt$ and $d\mathbf{C}/dt$ are the unknown nodal vectors of solution and time derivatives for the hydraulic head h and the concentration **C**, respectively; and **Y** and **Z** represent nodal vectors of length $(m-d)$ for the right-hand sides. The matrices **S**, **T**, **R**, **D** and **Q** are here of symmetric nature. On the other hand, the velocity-dependent convection matrix **K** is unsymmetric.

The elements of marices and vectors are given by (summation convention is used):

$$S_{kl} = \sum_e \int\int_{\Omega^e} S\, N_k N_l \, d\Omega \tag{A5a}$$

$$T_{kl} = \sum_e \left(\int\int_{\Omega^e} T_{ij} \frac{\partial N_k}{\partial x_i} \frac{\partial N_l}{\partial x_j} d\Omega - \int_{\Gamma_3^e} \Lambda_1 N_k N_l \, d\Gamma \right) \tag{A5b}$$

$$Y_k = \sum_e \left\{ - \int\int_{\Omega^e} N_k \left[\sum_{\nu=1}^{b} Q_B(x_\nu) \delta(x_1 - x_{1\nu}, x_2 - x_{2\nu}) - W \right] d\Omega \right.$$

$$\left. - \int_{\Gamma_2^e} N_k \, q_h^R d\Gamma - \int_{\Gamma_3^e} \Lambda_1 h_2^R N_k \, d\Gamma \right\} \tag{A5c}$$

$$R_{kl} = \sum_e \int\int_{\Omega^e} M\, R\, N_k N_l \, d\Omega \tag{A6a}$$

$$K_{kl} = \sum_e \int\int_{\Omega^e} N_k \left(N_\nu V_{i\nu} \frac{\partial N_l}{\partial x_i} + N_l \frac{\partial N_\nu}{\partial x_i} V_{i\nu} \right) d\Omega \tag{A6b}$$

$$D_{kl} = \sum_e \left(\int\int_{\Omega^e} n\tilde{D}_{ij} \frac{\partial N_k}{\partial x_i} \frac{\partial N_l}{\partial x_j} d\Omega - \int_{\Gamma_2^e} \Lambda_2 N_k N_l \, d\Gamma \right) \tag{A6c}$$

$$Q_{kl} = \sum_e \int\int_{\Omega^e} \left(R\, M\, \lambda_1 + S^* \frac{h_{t+\Delta t} - h_t}{\Delta t} \right) N_k N_l \, d\Omega \tag{A6d}$$

$$Z_k = \sum_e \left\{ \int\int_{\Omega^e} (-C'Q + C''W + nM\lambda_0) N_k N_l \, d\Omega \right.$$

$$\left. - \int_{\Gamma_2^e} N_k q_c^R d\Gamma - \int_{\Gamma_2^e} \Lambda_2 C_2^R N_k \, d\Gamma \right\} \tag{A6e}$$

To evaluate the coefficients of hydrodynamic dispersion a polynomial expansion of one order lower is used for the velocity components as

$$q_i = \sum \Psi_\nu(x_i) V_{i\nu}$$

where $\Psi_\nu(x_i)$ represents bilinear functions. Therefore one obtains for equation (A6c)

$$\tilde{D}_{ij} = (D_d M + \beta_T \tilde{V}) \delta_{ij} + (\beta_L - \beta_T)(\Psi_\nu V_{i\nu})(\Psi_\nu V_{j\nu}) / \tilde{V}$$

with

$$\tilde{V} = [(\Psi_\nu V_{i\nu})(\Psi_\nu V_{i\nu})]^{1/2}$$

The remaining system parameters in equations (A5) and (A6) are treated to be constant for each element. For the evaluation of the individual terms in equations (A5) and (A6) standard numerical integration based on a 3×3 Gaussian quadrature is used. To compute the "velocity" field **V** from derivative of the known field **H** using Darcy's law (6) as

$$V_{il} = -T_{ij} \frac{\partial N_k}{\partial x_j} H_k \qquad l,k = 1, \cdots, m \tag{A7}$$

a Gauss-point related evaluation is preferred for reasons of accuracy. For the numerically improved treatment of well singularities according to the local sink/source intensity Q of equation (11) singular well elements introduced by Charbeneau and Street (1979a,b) are utilized. It is achieved by a combination of an approximate solution $\tilde{h}$ with an analytic near-well function as

$$h \sim \tilde{h} + G \tag{A8}$$

where G represents a Green's function. Considering steady-state and isotropic ($T_{ij} = T\delta_{ij}$) conditions the singular well element corresponds to a circle with the radius R_s and the well at its centre. Then, the Green's function becomes

$$G = \frac{Q_B}{2\pi T} ln(\frac{R_s}{r}) \quad \text{with} \quad r = (x_i x_i)^{1/2} \tag{A9}$$

Integrating the well expressions in equation (A5c) under consideration of the analytical function valid over the singular well element the following sink/source contributions to nodes belonging to a well element are derived:

$$Y_k = -\frac{Q_B}{2\pi} \quad \text{if } k \text{ is mid-side node}$$

$$Y_k = = -\frac{Q_B}{2\pi}(\frac{\pi}{2} - 1) \quad \text{if } k \text{ is corner node} \tag{A10}$$

To solve numerically the systems of ordinary differential equations (A3) and (A4) a time-weighted difference approximation is used (Diersch 1981a) yielding

$$[\frac{\mathbf{S}}{\Delta t} + \mathbf{T}\sigma] \cdot \mathbf{H}_{t+\Delta t} = [\frac{\mathbf{S}}{\Delta t} - \mathbf{T}(1-\sigma)] \cdot \mathbf{H}_t + [\mathbf{Y}_{t+\Delta t}\sigma + (1-\sigma)\mathbf{Y}_t] \tag{A11}$$

and

$$[\frac{\mathbf{R}}{\Delta t} + (\mathbf{K} + \mathbf{D} + \mathbf{Q})\sigma] \cdot \mathbf{C}_{t+\Delta t}$$

$$= [\frac{R}{\Delta t} - (K + D + Q)(1 - \sigma)] \cdot C_t + [\sigma Z_{t+\Delta t} + (1 - \sigma)Z_t] \quad , \qquad (A12)$$

where Δt is the time-step and σ $(0 \leq \sigma \leq 1)$ corresponds to a time weighting factor. Specifying σ one obtains several time marching schemes, in particular

$\sigma = 0$ for explicit scheme

$\sigma = 1/2$ for Crank-Nicolson scheme

and $\sigma = 1$ for fully implicit scheme

To avoid oscillations the schemes have to require

$$\Delta t < \frac{1}{(1-\sigma)\ \mathbf{max}\ \omega_i} \quad , \qquad (A13)$$

which are restricted with regard to the time step Δt excluding the fully implict scheme ($\sigma = 1$), where ω_i represents the modal eigenvalues.

For the approximate solutions of hydraulic head h and concentration C an estimation of the global error norm gives accuracy of order

$$0(\Delta t^{\nu}, d^{\xi})$$

with

$$\nu = 1 \quad \text{for } \sigma \in (0,1)$$

$$\nu = 2 \quad \text{for } \sigma = 1/2$$

and

$$\xi = r \quad \text{for mid-side nodes}$$

$$\xi = 2r \quad \text{for corner nodes,}$$

where d is the characteristic element length and r indicates the order of interpolation ($r = 2$ for present study). The error $0(\Delta t)$ for the implicit scheme is inherently associated with greater influences regarding numerical dispersion. It can be shown for quasi one-dimensional consideration ($D_{ij} \rightarrow D_i \; q_i \rightarrow q$) an erroneous increasing of dispersion and dispersivity, respectively, by

$$D \rightarrow D + \Delta t \; q^2/2 - 0(d^r)$$

or

$$\beta_L \rightarrow \beta_L + \Delta t \; q/2 - 0(d^r)$$

Accordingly, a possibly small time step Δt should be used. The errors resulting from the finite element discretization are further discussed in Diersch (1983b). however, they can practically be neglected for higher orders of approximation ($r \geq 2$).

Using a Gauss-quadrature-point related evaluation for the "velocity" field according to equation (A7) superconvergent theoretical error estimates have been proven. As shown by Carey (1982) one obtains a local estimate of $0(d^{2r})$ for the derivatives at these points.

APPENDIX B: SUMMARY OF PHYSICAL PARAMETERS USED

Subregion	Transmissivity $T[m^2/s]$	Thickness $M[m]$	Porosity $n[1]$
1	$1.25 \cdot 10^{-2}$	35	0.3
2	$1.93 \cdot 10^{-2}$	42	0.3
3	$3.02 \cdot 10^{-2}$	38	0.3
4	$2.25 \cdot 10^{-2}$	56	0.3

$S(= S^*) = 0.2 \quad [1]$

$W = 10.5 \quad [mm/month]$

$Q_B = 1000. \quad [m^3/day]$

$\beta_L = 4 \quad [m]$

from history

$\beta_T = 0.4 \quad [m]$

$\kappa = 0.$

$\lambda_1 = \lambda_0 = 0.$

$C' = C'' = 0.$

APPENDIX C: NOMENCLATURE

Remark: If a symbol is used in another sense as listed below so it is noted in the text.

Symbol	Dimension	Explanation
A	(L^2T^{-1})	System matrix, Equations (18), (A11)
B	(L^2T^{-1})	System matrix, Equations (18), (A11)
b		Number of single wells
C	(ML^{-3})	Concentration
$\hat{C}$	(ML^{-3})	Vertical-averaged concentration, Equation (4)
C'	(ML^{-3})	Well-sink/source concentration
C''	(ML^{-3})	Accretion-related input concentration
C_1^R	(ML^{-3})	Dirichlet-type boundary concentration
C_2^R	(ML^{-3})	Cauchy-type boundary concentration
C_B^m	(ML^{-3})	Mean well mixing concentration, Equation (24)
C_H^m	(ML^{-3})	Contaminant mixing concentration of siphon well section (SWS), Equation (21)
C_{ref}	$(M\,L^{-3})$	Reference concentration
C	$(M\,L^{-3})$	Resulting nodal concentration vector
D_{ij}	(L^2T^{-1})	Tensor of hydrodynamic dispersion, Equation (3c)
$\bar{D}_{ij}$	$(L^{-3}T^{-1})$	Vertical-integrated dispersion tensor,

		Equation (13)
D_d	(L^2T^{-1})	Medium diffusion coefficient
$\mathbf{D}$	(L^3T^{-1})	Dispersion matrix, Equation (A6c)
d	(L)	Characteristic element length
$\mathbf{E}$	(L^3T^{-1})	System matrix, Equations (19), (A12)
e		Element number
e_j	(L^0)	Components of gravitational unit vector in x_j-direction
$\mathbf{F}$	$(M\ T^{-1})$	System vector, Equations (19), A12)
G	(L)	Green's function, Equation (A9)
$\mathbf{G}$	(L^3T^{-1})	System vector, Equations (18), (A11)
g	$(L\ T^{-2})$	Gravitational acceleration
$\mathbf{H}$	(L)	Resulting nodal vector of hydraulic head
h	(L)	Hydraulic head
$\hat{h}$	(L)	Vertical-averaged hydraulic head, similar to Equation (4)
h_1^R	(L)	Dirichlet-type boundary hydraulic head
h_2^R	(L)	Cauchy-type boundary hydraulic head
i,j		Indices
K_{ij}	$(L\ T^{-1})$	Tensor of hydraulic conductivity
$\mathbf{K}$	(L^3T^{-1})	Convection matrix, Equation (A6b)
k		Index
L_1,L_2,L_3	(L)	Circumference lengths of well galleries
l		Index
M	(L)	Aquifer thickness
m		Number of nodal points
N	(L^0)	Basis function
n	(L^0)	Kinematic porosity
n_0	(L^0)	Specific yield
n_i	(L^0)	Directional cosines
P_A	$(M\ T^{-1})$	Contaminant effluent entering the surface waters, Equation (22)
P_B	$(M\ T^{-1})$	Contaminant effluent by interception pumping wells, Equation (25)
P_{ref}	$(M\ T^{-1})$	Reference effluent
$\bar{q}_i$	(L^2T^{-1})	Specific Darcy volumetric flux,

		Equation (10)
q_c	$(M\ L^{-1}T^{-1})$	Normal concentration flux, Equation (17)
q_c^R	$(M\ L^{-1}T^{-1})$	Neumann-type boundary concentration flux
q_h	(L^2T^{-1})	Normal Darcy volumetric flux, Equation (17)
q_h^R	(L^2T^{-1})	Neumann-type boundary volumetric flux
Q	$(L\ T^{-1})$	Well function, Equation (11)
Q_B	(L^3T^{-1})	Well discharge pumped
Q_I	(L^3T^{-1})	Infiltration rate of recharge basin (hydraulic barrier)
Q_A	(L^3T^{-1})	Pumping capacity of gallery A
Q_B	(L^3T^{-1})	Pumping capacity of gallery B
$\mathbf{Q}$	(L^3T^{-1})	Source matrix, Equation (A6d)
R	(L^0)	Retardation factor, Equation (9)
R_s	(L)	Radius of singular well element
$\mathbf{R}$	(L^3)	Retardation matrix, Equation (A6a)
r	(L)	Radial coordinate
S, S^*	(L^0)	Aquifer storage coefficients, Equation (8)
S_s	(L^{-1})	Specific storage coefficient, Equation (1b)
$\mathbf{S}$	$(M\ L^0)$	Storage matrix, Equation (A5a)
s	(ML^{-3})	Sorbed concentration
T_{ij}	(L^2T^{-1})	Tensor of transmissivity, Equation (12)
T	(L^2T^{-1})	Isotropic transmissivity
$\mathbf{T}$	(L^2T^{-1})	Transmissivity matrix, Equation (A5b)
t	(T)	Elapsed time
Δt	(T)	Time step
U	(L)	Circumference length
v_i	$(L\ T^{-1})$	Components of average pore velocity
$\hat{v}_i$	$(L\ T^{-1})$	Vertical-averaged pore velocity, similar to Equation (4)
V	$(L\ T^{-1})$	Absolute pore velocity
$\bar{V}$	(L^2T^{-1})	Absolute specific volumetric flux
$\mathbf{V}$	(L^2T^{-1})	Resulting nodal vector of "velocity"
W	$(L\ T^{-1})$	Groundwater accretion

$\mathbf{W}$	(L^3T^{-1})	System matrix, Equations (19), (A12)
x_i	(L)	Spatial coordinates
x_{il}	(L)	Spatial coordinates of point l
x_3	(L)	Vertical coordinate
$\mathbf{Y}$	(L^3T^{-1})	Boundary vector, Equation (A5c)
$\mathbf{Z}$	$(M\ T^{-1})$	Boundary vector, Equation (A6e)
α	(1)	Skeleton compressibility
β	(1)	Groundwater compressibility
β_L	(L)	Longitudinal dispersivity
β_T	(L)	Transversal dispersivity
Γ	(L)	Boundary circumference line
$\Gamma_1, \ldots, \Gamma_6$	(L)	Boundary sections on which boundary conditions are specified
Γ^e	(L)	Element boundary
$\delta()$	(L^{-2})	Dirac delta function
δ_{ij}	(1)	Kronecker tensor
κ	(1)	Linear sorption coefficient
Λ_1	$(L\ T^{-1})$	Colmation coefficient describing the aquifer-surface waters interactions
Λ_2	(L^2T^{-1})	Concentration transfer coefficient
λ_0	$(M\ L^{-3}T^{-1})$	Source/sink of concentration
λ_1	(T^{-1})	Concentration decay rate
ν		Index
ξ		order of approximation
ρ	$(M\ L^{-3})$	Groundwater density
ρ_0	$(M\ L^{-3})$	Reference groundwater density
σ	(1)	Time-weighting coefficient ($0 \leq \sigma \leq 1$)
Ψ	(L^0)	Dispersion related polynomial expansion for velocity
Ω	(L^2)	Two-dimensional (horizontal) study area
Ω^e	(L^2)	Area of finite element
ω_i	(T^{-1})	Modal eigenvalues

Special notations and abbreviations

$\hat{}$ Vertical averaging

$\bar{}$ Vertical integrating

$\sum_{e}$ sum over all elements (asssembly process)

CB Ceasing barrier

OB Operating barrier

SWS Siphon well section (exposed part of well gallery *A*)

REFERENCES

Bear, J. 1972. Dynamics of Fluids in Porous Media. American Elsevier, New York.

Bear, J. 1979. Hydraulics of Groundwater. McGraw-Hill, London.

Beims, U. 1984. Auswertung von Güterpumpversuchen. *Zeitschrift für Angewandte Geologie* (forthcoming).

Bertsch, W. 1978. Die Koeffizienten der longitudinalen und transversalen hydrodynamischen Dispersion — ein Literaturüberblick. *Deutsche Gewässerkundliche Mitteilungen* 22(2):37-46.

Bredehoeft, J.D., and G.F. Pinder. 1973. Mass transport in flowing groundwater. *Water Resources Research* 9(1):194-210.

Bruch, Jr., J.C. 1970. Two-dimensional dispersion experiments in a porous medium. *Water Resources Research* 6(3):791-800.

Carey, G.F. 1982. Derivative calculation from finite element solutions. *Computer Methods in Applied Mechanics and Engineering* 35:1-14.

Charbeneau, R.J., and R.L. Street. 1979a. Modeling groundwater flow fields containing point singularities: a technique for singularity removal. *Water Resources Research*, 15(3):583-594.

Charbeneau, R.J. and R.L. Street. 1979b. Modeling groundwater flow fields containing point singularities: streamlines, travel times, and breakthrough curves. *Water Resources Research*, 15(6):1445-1450.

Dagan, G. 1983. Stochastic modeling of solute transport by groundwater flow. Paper presented at the symposium "Relation of Groundwater Quantity and Quality of the IAHS", Hamburg, August 1983.

Das Gupta, A., and P.N.D.D. Yapa. 1982. Saltwater Encroachment in an Aquifer: A Case Study. *Water Resources Research*, 18(3):546-556.

Diersch, H.-J. 1979. Finite-Element-Modellierung instationärer zweidimensionaler Stofftransportvorgänge im Grundwasser. Beiträge zur

wissenschaftlichen Konferenz "Simulation der Migrationsprozesse im Boden- und Grundwasser". Technische Universität Dresden, Vol. 1, 126-138.

Diersch, H.-J. 1980a. Finite-Element-Programssystem FEFLOW. Program description. Institut für Mechanik der AdW der DDR, Berlin.

Diersch, H.-J. 1980b. Mehrphasiger Stoff-, Impuls- und Wärmetransport im ungesättigten und gesättigten porösen Medium. *Acta Hydrophysica*, 25(4):351-407.

Diersch, H.-J. 1981a. Finite-Element-Galerkin-Modell zur Simulation zweidimensionaler konvektiver und dispersiver Stofftransportprozesse im Boden. *Acta Hydrophysica*, 26(1):5-44.

Diersch, H.-J. 1981b. Study of free convective flows in porous media and effects of mechanical dispersion using finite element methods. *Gerlands Beiträge zur Geophysik*, 90(6):489-506.

Diersch, H.-J. 1981c. Primitive variable finite element solutions of free convection flows in porous media. *Zeitschrift für Angewandte Mathematik und Mechanik (ZAMM)*, 61(7):325-337.

Diersch, H.-J., and P. Nillert. 1983a. Modelluntersuchungen zu vorbeugenden Massnahmen gegen Schadstoffhavarien an Uferfiltratfassungen. *Wasserwirtschaft-Wassertechnik*, 33(3):93-104.

Diersch, H.-J. 1983b. On finite element upwinding and its numerical performance in simulating coupled convective transport processes. *Zeitschrift für Angewandte Mathematik und Mechanik (ZAMM)*, 63(10):479-488.

Diersch, H.-J., G. Nützmann, and H. Scholz. 1983c. Modellierung und numerische Simulation geohydrodynamischer Transportprozesse. 1 Theorie. Preprint P-MECH-06/83. Institut für Mechanik der AdW der DDR, Berlin, p. 47.

Diersch, H.-J., D. Prochnow, and M. Thiele. 1984a. Finite element analysis of dispersion-affected saltwater upconing below a pumping well. *Applied Mathematical Modelling* (forthcoming).

Diersch, H.-J., and P. Nillert. 1984b. Untersuchungen zur Dynamik geogen bedingter Salzkontaminationen an Vertikalfilterbrunnen. *Zeitschrift für Angewandte Geologie*, 30(2):97-108.

Enquist, B., and H.-O. Kreiss. 1979. Difference and finite element methods for hyperbolic differential equations. *Computer Methods in Applied Mechanics and Engineering*, 17/18:581-596.

Fried, J.J. 1975. Groundwater pollution. Elsevier, Amsterdam.

van Genuchten, M.Th., and W.J. Alves. 1982. Analytical solutions of the one-dimensional convective-dispersive solute transport equation. *Technical Bulletin*, No. 1661, US Department of Agriculture, Agriculture Research Service, Washington, DC.

Gorelick, S.M. 1983. A Review of Distributed Parameter Groundwater Management Modeling Methods. *Water Resources Research*, 19(2):305-319.

Gray, W.G., and J.L. Hoffman. 1981. A numerical model study of the contaminant plume emanating from Price's landfill in Egg Harbor Township, New Jersey. Princeton Water Resources Program Report, 81-WR-8, Princeton University, p. 93.

Gray, W.G. 1982. Derivation of vertically averaged equations describing multiphase flow in porous media. *Water Resources Research*, 18(6):1705-1712.

Hassanizadeh, M., and W.G. Gray. 1979. General conservation equations for

multi-phase systems: 1. Averaging procedure. *Advances in Water Resources*, 2(3):131-144.

Hibsch, G., and A. Kreft. 1979. Determination of aquifer transport parameters. *Journal of the Hydraulics Division*, Proceedings of the ASCE, 105(HY9):1137-1151.

Jackson, R.E. et al. 1980. Aquifer contamination and protection. UNESCO Studies and Reports in Hydrology, No. 30.

Klotz, D. 1982a. Abhängigkeit der longitudinalen Dispersion von Parametern des Grundwassers und des Grundwasserleiters. GSF-Bericht R 290. Gesellschaft für Strahlen- und Umweltforschung mbH, München, 309-322.

Klotz, D. 1982b. Abhängigkeit der transversalen Dispersion von Parametern des Grundwassers und des Grundwasserleiters. GSF-Bericht R 290. Gesellschaft für Strahlen- und Umweltforschung mbH, München, 340-349.

Konikow, L.F. 1977. Modeling chloride movement in the alluvial aquifer at the Rocky Mountain Arsenal, Colorado. Geological Survey Water-Supply Paper 2044, Washington, p. 43.

Lavrik, W.I. and A.F. Miljustin. 1978. Analytic and numerical-analytic solutions of two-dimensional mass transport problems in groundwater (in Russian). Institute for Mathematics, Academy of Sciences of the USSR, Kiev, Preprint 78-24, p. 54.

Mohsen, M.F.N., G.J. Farquar, and N. Kouwen. 1978. Modelling methane migration in soil. *Applied Mathematical Modelling*, 2:294-301.

Pickens, J.F., and W.C. Lennox. 1976. Numerical simulation of waste movement in steady groundwater flow systems. *Water Resources Research*, 12(2):171-180.

Pickens, J.F., and G.E. Grisak. 1981a. Scale-dependent dispersion in a stratified granular aquifer. *Water Resources Research*, 17(4):1191-1211.

Pickens, J.F., and G.E. Grisak. 1981b. Modeling of scale-dependent dispersion in hydrologic systems. *Water Resources Research*, 17(6):1701-1711.

Pinder, G.F. 1973. A Galerkin-finite element simulation of groundwater contamination on Long Island, New York. *Water Resources Research*, 9(6):1657-1669.

Pinder, G.F. and W.G. Gray. 1977. Finite Element Simulation in Surface and Subsurface Hydrology. Academic Press, New York.

Sauty, J.-P. 1980. An analysis of hydrodispersive transfer in aquifers. *Water Resources Research*, 16(1):145-158.

Scholz, H. 1982. Ableitung von Modellgleichungen zur horizontalebenen Beschreibung von Stofftransportvorgängen im Grundwasser. Preprint P-MECH-09/82. Institut für Mechanik der AdW der DDR, Berlin, p. 38.

Segol, G., and G.F. Pinder. 1976. Transient simulation of saltwater intrusion in southeastern Florida. *Water Resources Research*, 12(1):65-70.

Smith, L., and F.W. Schwartz. 1980. Mass transport 1. A stochastic analysis of macroscopic dispersion. *Water Resources Research*, 16(2):303-313.

Stoyan, G. 1979. On a maximum norm stable, monotone and conservative difference approximation of the one-dimensional diffusion-convection equation. Beiträge zur wissenschaftlichen Konferenz "Simulation der Migrationsprozesse im Boden- und Grundwasser", Technische Universität Dresden, Vol. 1, 137-158.

Tang, D.H., F.W. Schwartz, and L. Smith. 1982. Stochastic modeling of mass

transport in a random velocity field. *Water Resources Research*, 18(2):231-244.

Voigt, H.D., and F. Häfner. 1984. Grundlagen des Stoff- und Wärmetransportes in porösen Schichten. *Zeitschrift für Angewandte Geologie* (forthcoming).

Wood, E.F., R.A. Ferrera, W.G. Gray, and G.F. Pinder. 1984. Groundwater Contamination from Hazardous Wastes. Prentice Hall, Inc., Engelwood Cliffs.